

LCLS-II Undulator Segment Measurement Results

SXU-011

SLAC Traveler for LCLS-II SXU Segment Measurement Results

This traveler is intended to document the checking the final magnetic measurements of an Undulator Segment performed on the Kugler bench in the Magnetic Measurement Facility (MMF) at SLAC after the completion of the tuning process. It contains basic performance indicators compared against tolerances as well as documentary information both in graphical and textual representation.

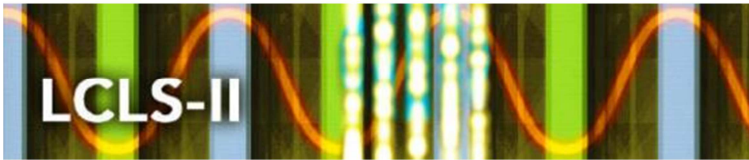
Serial number from magnet label:	29A804-011
Device name from magnet label:	SXU-011

Measurement Procedure:

The measurements have been carried out after the undulator segment had been fully tuned according to “LCLS-II Undulator Test Plan” (LCLS-TN-17-1).

Evaluation of Hall Probe Scans: Data Listings A

MATLAB function "EvaluateUndulatorField" on	8/20/2018 18:08	
A. SCAN PARAMETERS		
Serial Number	29A804-011	
Device Name	SXU-011	
z Scanning Date & Time Range	08/14/2018 15:11 - 08/15/2018 06:56	
Undulator Temperature	20.0982± 0.0050	°C
Room Temperature	20.1082± 0.0081	°C
x axis position	0.076032	m
y axis position	0.000156	m
Total number of poles per strongback	174	
Number of full field poles	168	
Number of core poles	162	
First core pole #	8	
Last core pole #	167	
Average λ_u	39.002	mm
RMS λ_u	24.2	μ m
Scans averaged	3	
Tuning Gap	10.001	mm
Commissioning Gap	10.391	mm



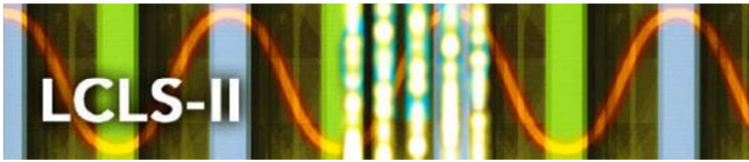
Evaluation of Hall Probe Scans at Tuning Gap: Data Listings B

MATLAB function "EvaluateUndulatorField" on	8/20/2018 18:08	
B. CORE EVALUATIONS FOR TUNING GAP		
Tuning Gap Scanning Date & Time	8/14/2018 19:54	
Tuning Gap Temperature	20.10± 0.04	°C
Planar Hall Effect Correction Range	0.790800 - 4.101000	m
Planar Hall Effect x Corr Function	-0.38 G + (z - 0.790800 m) * 0.14 G/m	
Planar Hall Effect y Corr Function	-0.38 G + (z - 0.790800 m) * 0.26 G/m	
Coil Range	0.645945 - 4.245945	m
< λ_u >	39.002± 0.002	mm
< k_u >	161.10± 0.01	1/m
< K_u >	4.225± 0.000	
< K_{eff} > @ Tuning Temperature	4.22434± 0.00004	
< L_{eff} >	3.31358± 0.00006	m
< $L_{2\pi}$ >	0.38700± 0.00002	m
I1X (Cell Range Total)	20.15	μTm
I2X (Cell Range Total)	67.64	μTm^2
I1Y (Cell Range Total)	-8.04	μTm
I2Y (Cell Range Total)	-2.2	μTm^2
PI (Cell Range Total)	85,898.20	T^2mm^3
Phase Shake	1.05	degXray
Cell Phase Advance (over 4.400000 m)	31,596.0 (88×360-84.0)	degXray
Undulator Entrance Phase	1218.4± 0.1	degXray
Undulator Exit Phase	1217.6± 0.1	degXray
Undulator Phase Imbalance: Entrance - Exit	0.8± 0.1	degXray
Cell Entrance min. Phase Shifter Correction	221.6	degXray
Cell Exit min. Phase Shifter Correction	222.4	degXray



Evaluation of Hall Probe Scans at Commissioning Gap: Data Listings C

MATLAB function "EvaluateUndulatorField" on	8/20/2018 18:08	
C. CORE EVALUATIONS FOR COMMISSIONING GAP		
Commissioning Gap Scanning Date & Time	8/15/2018 7:05	
Commissioning Gap Temperature	20.10± 0.04	°C
Planar Hall Effect Correction Range	0.790800 - 4.101000	m
Planar Hall Effect x Corr Function	-0.39 G + (z - 0.790800 m) * 0.14 G/m	
Planar Hall Effect y Corr Function	-0.38 G + (z - 0.790800 m) * 0.26 G/m	
Coil Range	0.645948 - 4.245948	m
<λ _u >	39.002± 0.002	mm
<k _u >	161.10± 0.01	1/m
<K _u >	4.050± 0.000	
<K _{eff} > @ Tuning Temperature	4.05004± 0.00004	
<L _{eff} >	3.31411± 0.00006	m
<L _{2π} >	0.35887± 0.00002	m
I1X (Cell Range Total)	19.63	μTm
I2X (Cell Range Total)	62.38	μTm ²
I1Y (Cell Range Total)	-3.11	μTm
I2Y (Cell Range Total)	15.77	μTm ²
PI (Cell Range Total)	78,968.40	T ² mm ³
Phase Shake	1.09	degXray
Cell Phase Advance (over 4.400000 m)	31,679.5 (88×360-0.5)	degXray
Undulator Entrance Phase	1260.2± 0.1	degXray
Undulator Exit Phase	1259.3± 0.1	degXray
Undulator Phase Imbalance: Entrance - Exit	0.9± 0.1	degXray
Cell Entrance min. Phase Shifter Correction	179.8	degXray
Cell Exit min. Phase Shifter Correction	180.7	degXray



Undulator Encoder Settings: Data Listings D

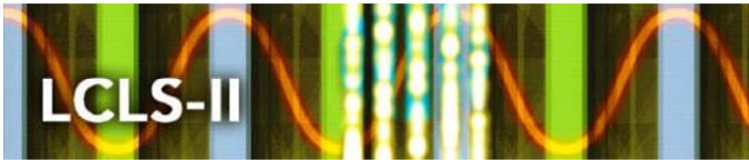
MATLAB function "EvaluateUndulatorField" on	8/20/2018 18:08	
D. ENCODER SETTINGS		
Upstream Gap Encoder Gain	-19,999.8±2.6	
Upstream Scaled Gap Encoder Offset	228.318±0.0000	mm
Downstream Gap Encoder Gain	-20,000.2±2.9	
Downstream Scaled Gap Encoder Offset	228.622±0.0000	mm
Upstream Scaled Top Motor Encoder Offset	-1015.516±0.000	mm
Downstream Scaled Top Motor Encoder Offset	-1015.168±0.000	mm

Undulator Capacitive Sensor Values: Data Listings E

E. CAPACITIVE SENSOR VALUES

Module	Pole	Capacitive Sensor Gap	Upstream Encoder	Downstream Encoder	
2	3/4	46.7139	46.6999	46.7000	mm
2	13/14	46.7109	46.6999	46.6999	mm
4	39/40	46.7088	46.6999	46.6999	mm
4	49/50	46.7131	46.6999	46.6999	mm

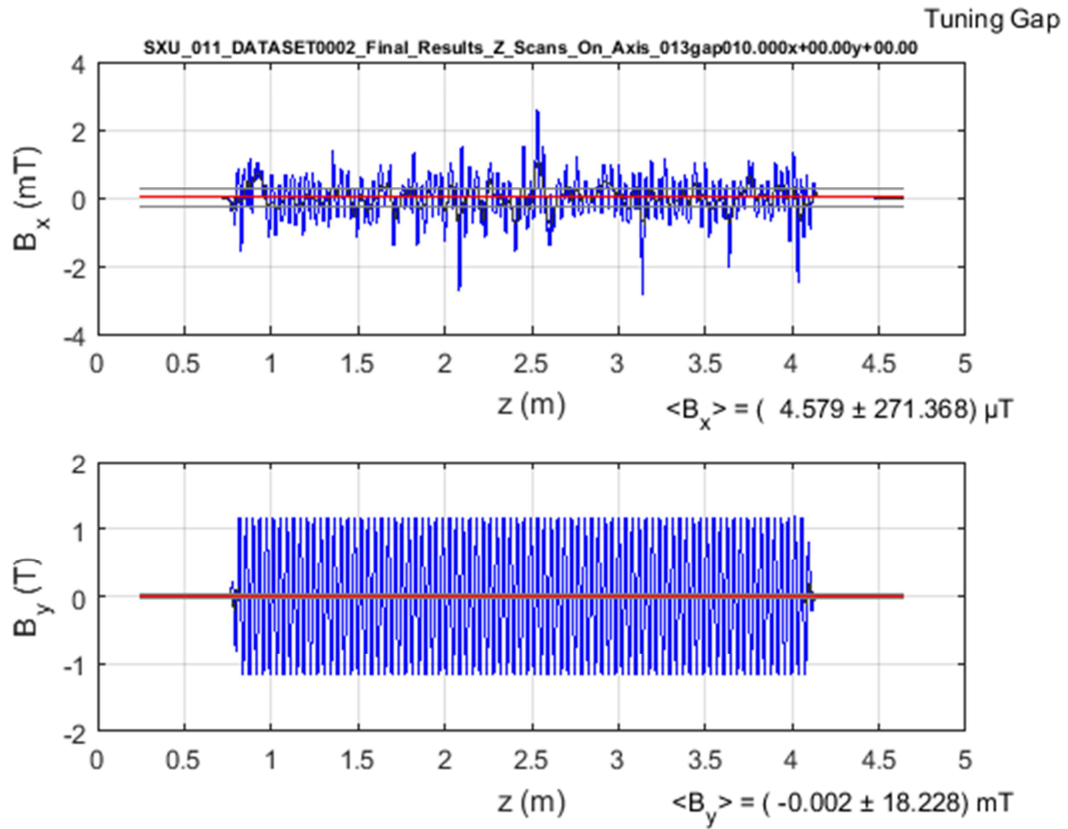
The following figures show result of the field analysis at the tuning gap.



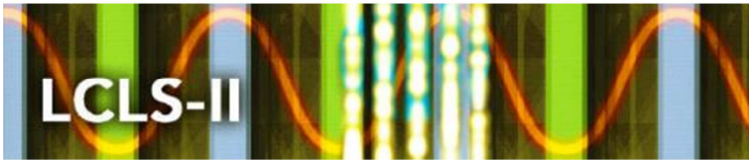
LCLS-II Undulator Segment Measurement Results

SXU-011

Evaluation of Hall Probe at Tuning Gap: B_x & B_y Plot



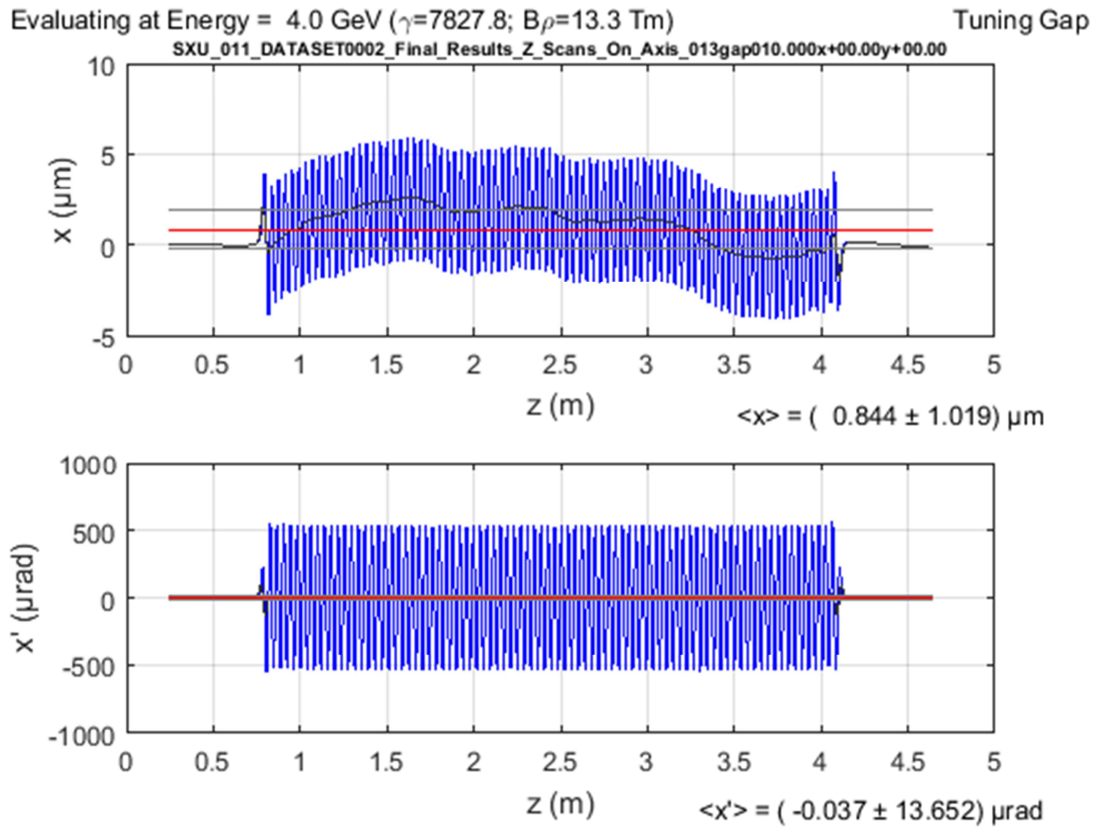
The figures show the x (upper) and y (lower) field components along the undulator tuning axis for the tuning gap. A running wiggler-period-average function is plotted in black (not very well visible in the lower figure). The horizontal lines indicate the mean (center red line) and the rms deviations from the mean (two black lines above and below the average) of that wiggler-period-average function. The corresponding mean and rms values are also printed on the right hand side underneath each figure. [Documentary Information]



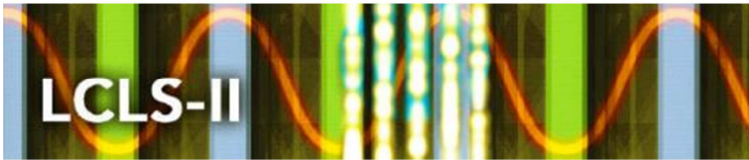
LCLS-II Undulator Segment Measurement Results

SXU-011

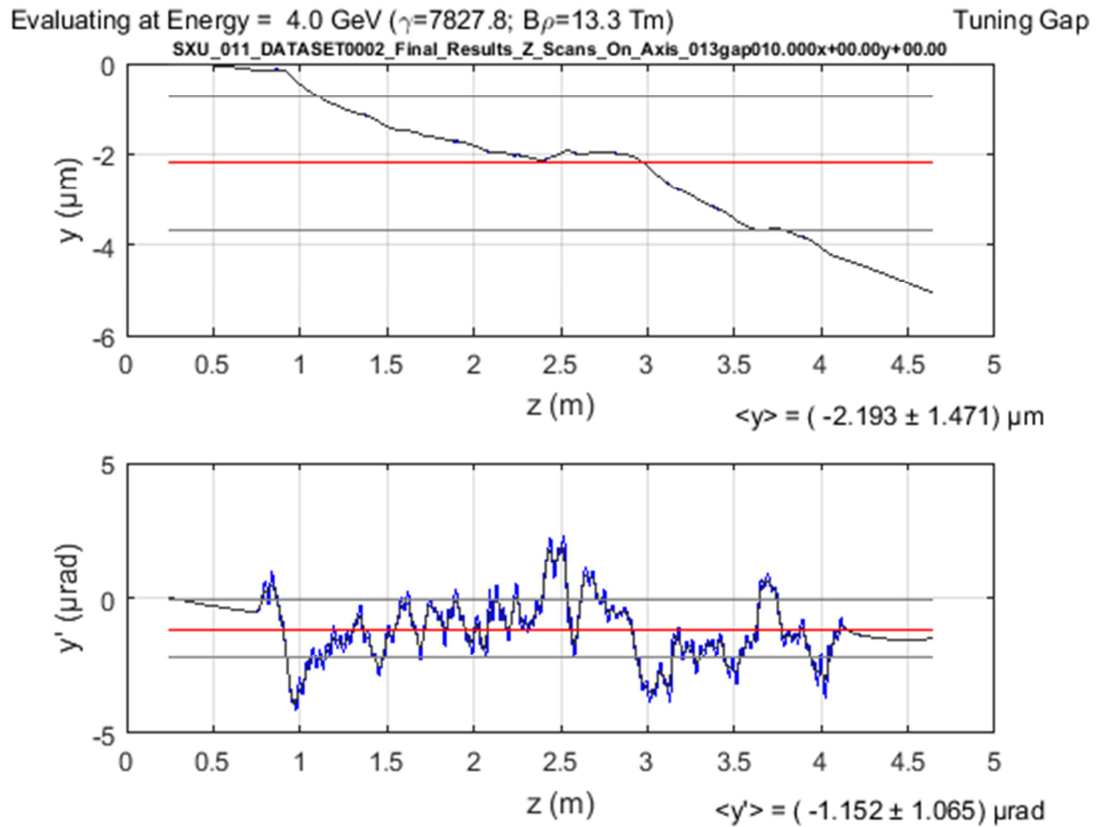
Evaluation of Hall Probe at Tuning Gap: x & x' Plot



The figures show the x (upper) and x' (lower) electron beam trajectories along the undulator tuning axis for the tuning gap based on the measured magnetic field components and estimated for an electron beam energy of 4.0 GeV. A running wiggler-period-average function is plotted in black (difficult to see in the lower figure). The horizontal lines indicate the mean (center red line) and the rms deviations from the mean (two black lines above and below the average) of that wiggler-period-average function. The corresponding mean and rms values are also printed on the right hand side underneath each figure. [Documentary Information]



Evaluation of Hall Probe Scans at Tuning Gap: y & y' Plot



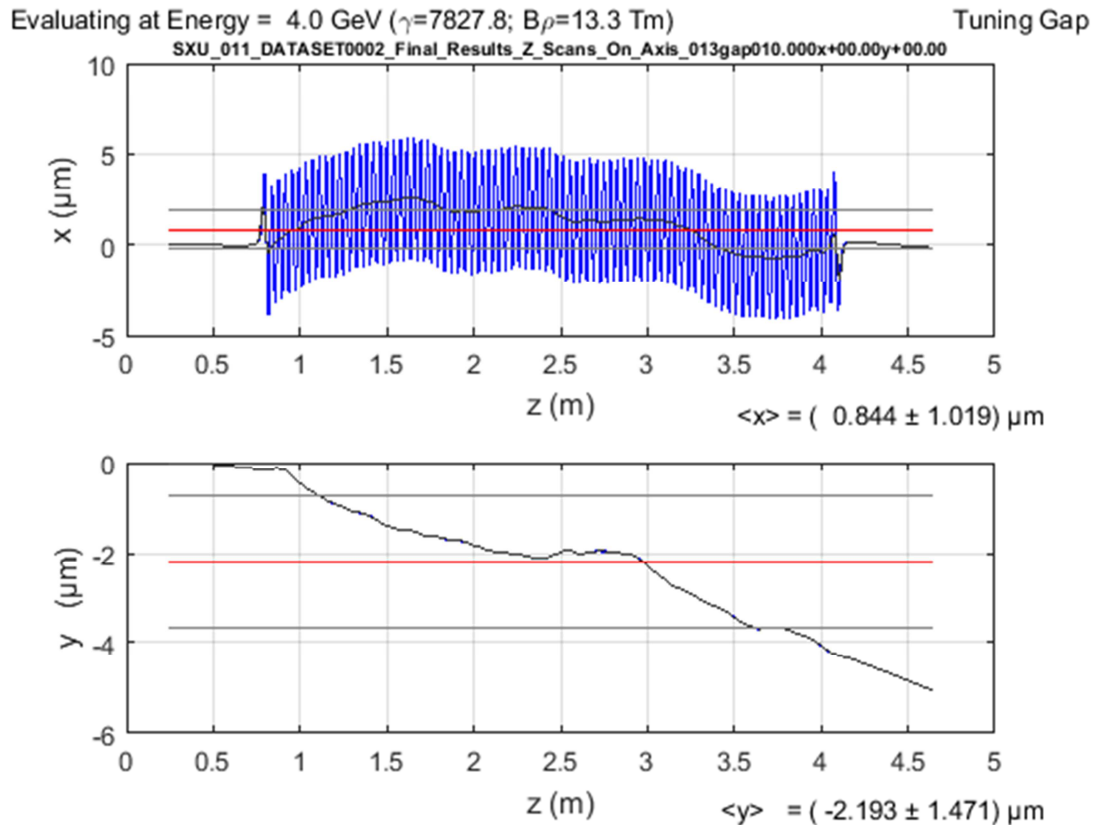
The figures show the y (upper) and y' (lower) electron beam trajectories along the undulator tuning axis for the tuning gap based on the measured magnetic field components and estimated for an electron beam energy of 4.0 GeV. A running wiggler-period-average function is plotted in black (difficult to see). The horizontal lines indicate the mean (center red line) and the rms deviations from the mean (two black lines above and below the average) of that wiggler-period-average function. The corresponding mean and rms values are also printed on the right hand side underneath each figure. [Documentary Information]



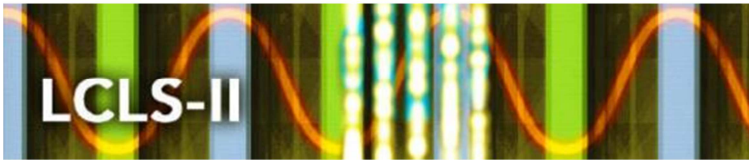
LCLS-II Undulator Segment Measurement Results

SXU-011

Evaluation of Hall Probe Scans at Tuning Gap: x & y Plot



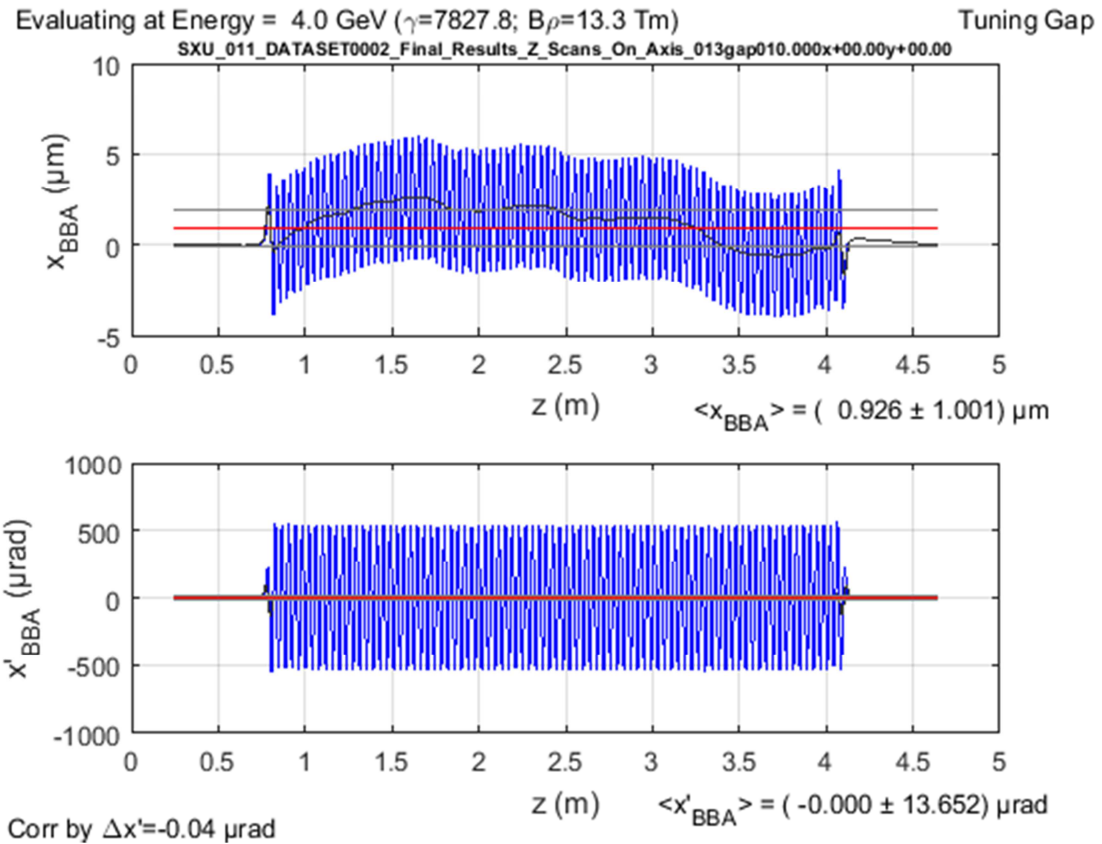
The figures show the x (upper) and y (lower) electron beam trajectories along the undulator tuning axis for the tuning gap based on the measured magnetic field components and estimated for an electron beam energy of 4.0 GeV. A running wiggler-period-average function is plotted in black (identical with the trajectory in the lower figure). The horizontal lines indicate the mean (center red line) and the rms deviations from the mean (two black lines above and below the average) of that wiggler-period-average function. The corresponding mean and rms values are also printed on the right hand side underneath each figure. [Documentary Information]



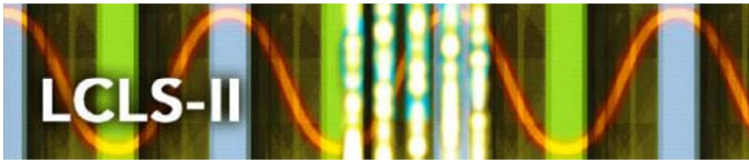
LCLS-II Undulator Segment Measurement Results

SXU-011

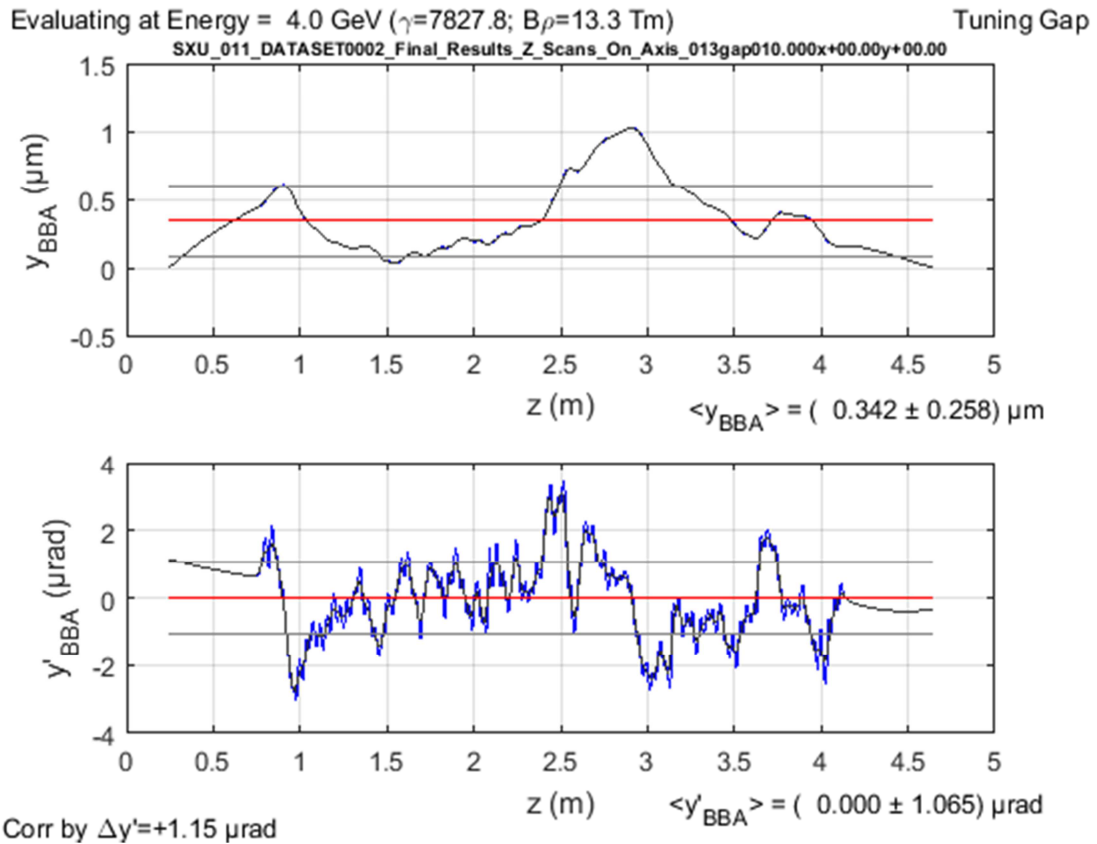
Evaluation of Hall Probe plus BBA correction at Tuning Gap: x & x' Plot



The figures show the x (upper) and x' (lower) electron beam trajectories along the undulator tuning axis for the tuning gap based on the measured magnetic field components after BBA correction (to zero the amplitudes at the cell boundaries) and estimated for an electron beam energy of 4.0 GeV. A running wiggler-period-average function is plotted in black (difficult to see in the lower figure). The horizontal lines indicate the mean (center red line) and the rms deviations from the mean (two black lines above and below the average) of that wiggler-period-average function. The corresponding mean and rms values are also printed on the right hand side underneath each figure. The amount of BBA correction applied is printed underneath the lower left corner of the lower figure. [Documentary Information]



Evaluation of Hall Probe plus BBA correction at Tuning Gap: y & y' Plot



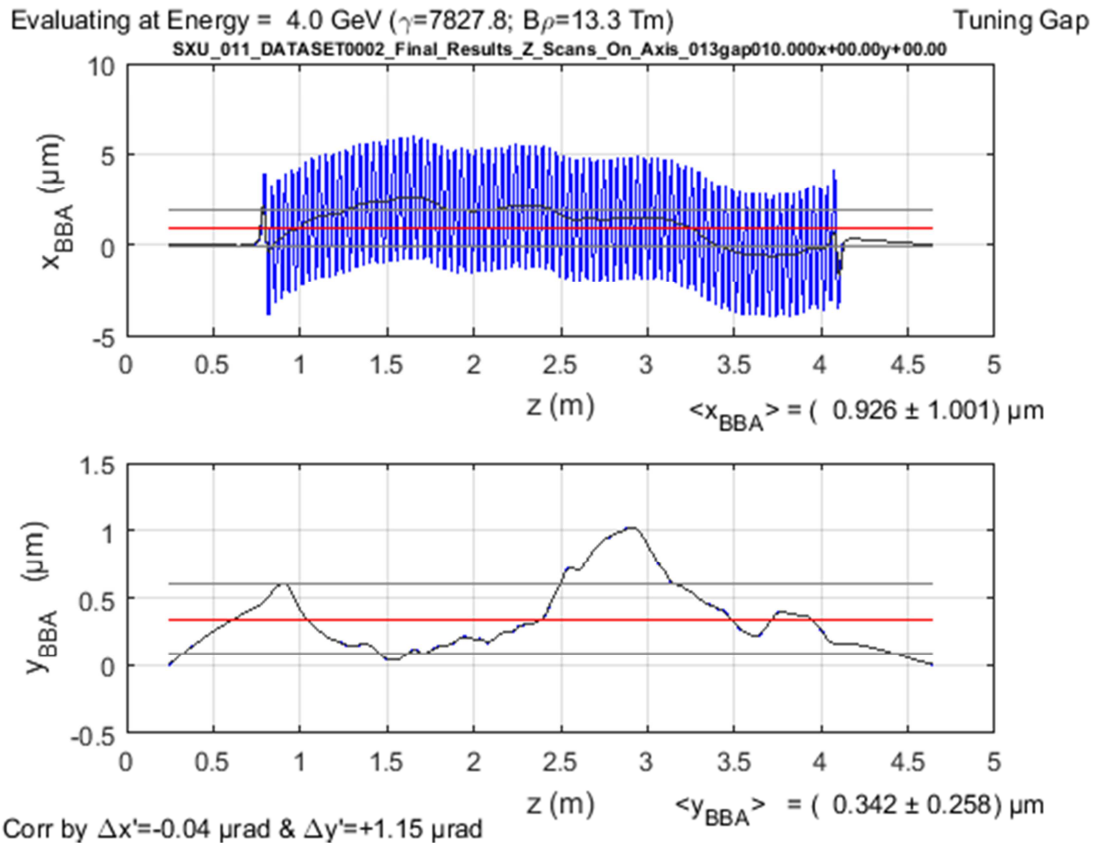
The figures show the y (upper) and y' (lower) electron beam trajectories along the undulator tuning axis for the tuning gap based on the measured magnetic field components after BBA correction (to zero the amplitudes at the cell boundaries) and estimated for an electron beam energy of 4.0 GeV. A running wiggler-period-average function is plotted in black (identical with the trajectories). The horizontal lines indicate the mean (center red line) and the rms deviations from the mean (two black lines above and below the average) of that wiggler-period-average function. The corresponding mean and rms values are also printed on the right hand side underneath each figure. The amount of BBA correction applied is printed underneath the lower left corner of the lower figure. [Documentary Information]



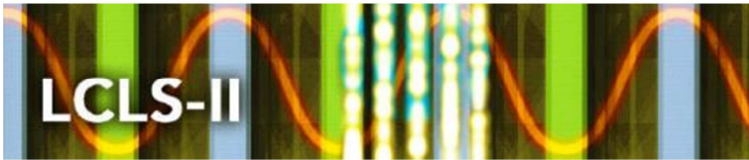
LCLS-II Undulator Segment Measurement Results

SXU-011

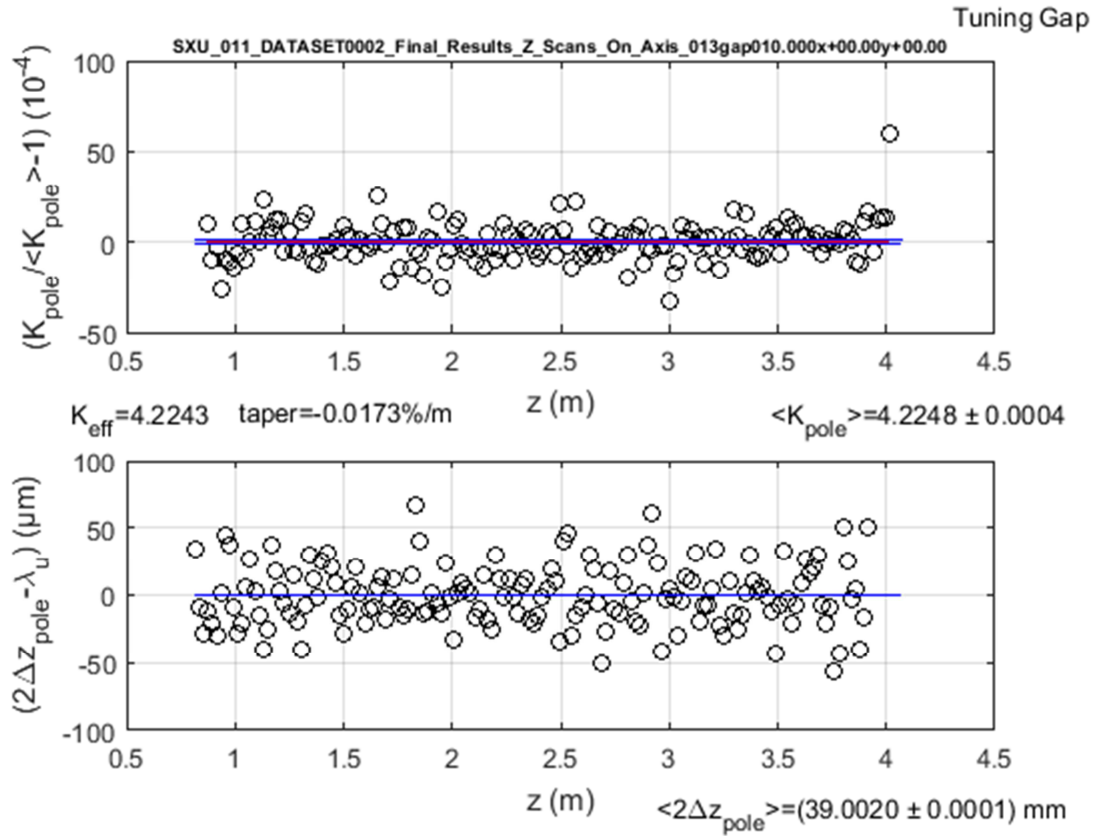
Evaluation of Hall Probe plus BBA correction at Tuning Gap: x & y Plot



The figures show the x (upper) and y (lower) electron beam trajectories along the undulator tuning axis for the tuning gap based on the measured magnetic field components after BBA correction (to zero the amplitudes at the cell boundaries) and estimated for an electron beam energy of 4.0 GeV. A running wiggler-period-average function is plotted in black (identical with the trajectory in the lower figure). The horizontal lines indicate the mean (center red line) and the rms deviations from the mean (two black lines above and below the average) of that wiggler-period-average function. The corresponding mean and rms values are also printed on the right hand side underneath each figure. The amount of BBA correction applied is printed underneath the lower left corner of the lower figure. [Documentary Information]

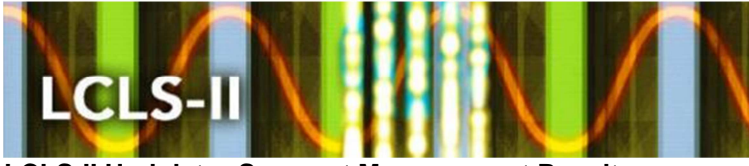


Evaluation of Hall Probe at Tuning Gap: K and λ_u variations



The figures show the per-pole undulator strength K_{pole} (upper) and the deviation of the pole width from the expected value of $\lambda_u/2$ (lower) for the 162 core undulator poles for the tuning gap. The horizontal lines indicate the mean (center red line) and the rms deviations from the mean (two black lines above and below the average). The corresponding mean and rms values are also printed on the right hand side underneath each figure. [Documentary Information]

For description of K calculation see next page.



LCLS-II Undulator Segment Measurement Results

SXU-011

K calculation description for previous page:

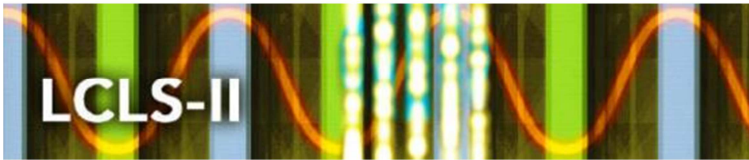
The undulator parameter, K_{pole} , in the upper figure, is calculated for each of the core poles based on the scanned vertical field values $B_y(z)$ as well as an interpolation of the upstream, $z_{0-dn,pole}$, and downstream, $z_{0-up,pole}$, field zero crossing locations using the following formula:

$$K_{pole}(z_{pole}) = \frac{\Delta z_{pole}}{2\pi} \frac{e}{m_e c} \sqrt{\frac{2}{\Delta z_{pole}} \int_{z_{0-up,pole}}^{z_{0-dn,pole}} B_Y^2(\hat{z}) d\hat{z}}$$

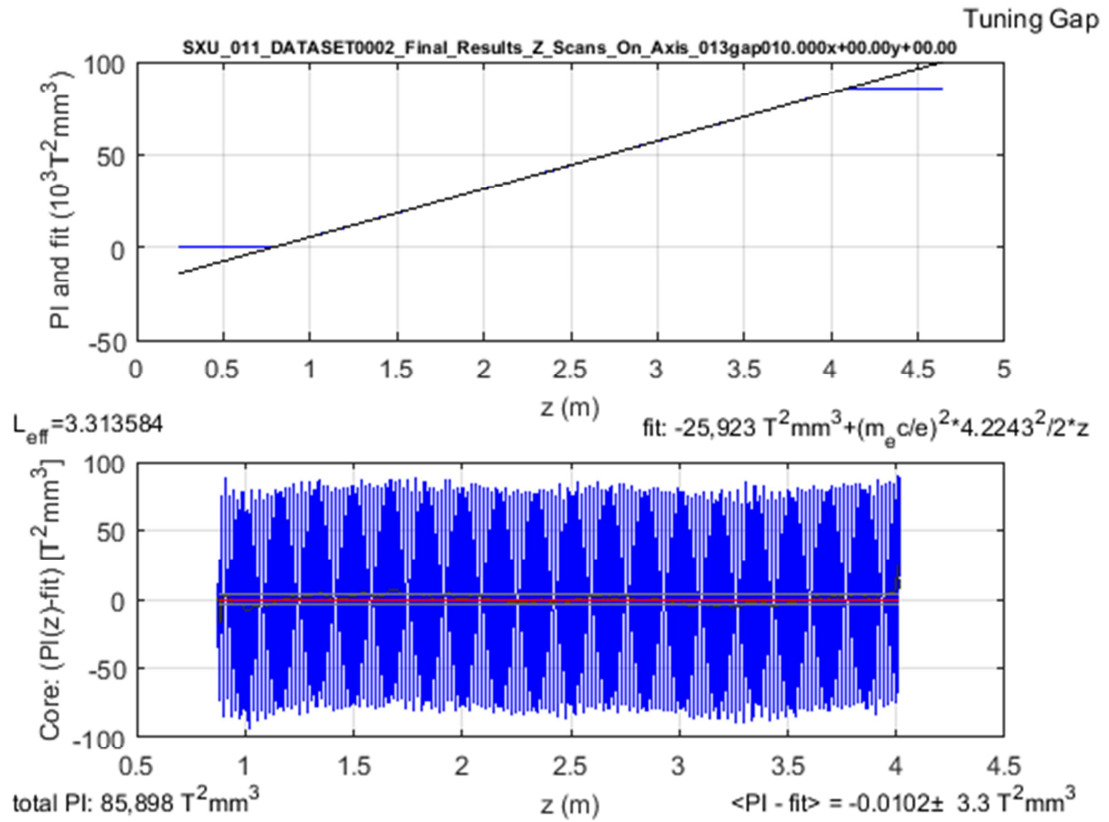
The term $\frac{e}{m_e c}$ uses the electron mass, m_e , the speed of light, c , and the electron's electric charge, e . The variable Δz_{pole} stands for

$$\Delta z_{pole} = z_{0-dn,pole} - z_{0-up,pole}$$

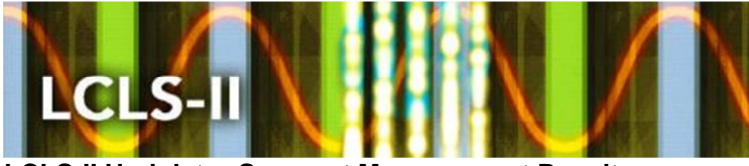
$$z_{pole} \approx \frac{1}{2} (z_{0-dn,pole} + z_{0-up,pole})$$



Evaluation of Hall Probe Scans for Tuning Gap: Phase Integral Plot



A description of the figure is given on the next page:



LCLS-II Undulator Segment Measurement Results

SXU-011

Figure description for previous page:

The upper figure shows the phase integral of an electron calculated from the measured on-axis magnetic field components for the tuning gap:

$$PI(z) = \int_0^z BL_{x1}^2(\hat{z}) d\hat{z} + \int_0^z BL_{y1}^2(\hat{z}) d\hat{z}$$

with

$$BL_{x1,y1}(z) = \int_0^z B_{x,y}(\hat{z}) d\hat{z} - \frac{1}{L} \int_0^L \left\{ \int_0^{\hat{z}} B_{x,y}(\hat{z}) d\hat{z} \right\} d\hat{z}$$

The function

$$\bar{PI}(z) = \bar{PI}(0) + z \left(\frac{m c}{e} \right)^2 \frac{1}{2} K_{eff}^2,$$

fitted to the measured phase integral $PI(z)$ with fit coefficients $\left(\frac{m c}{e} \right)^2 \frac{1}{2} K_{eff}^2$ and, can be seen as a straight black line in the upper plot. The values of the fit coefficients are printed at the right hand side underneath the upper figure. On the lower left of the upper figure the effective undulator length is printed, which is obtained as the distance over the undulator core, where the blue and black lines in the plot are on top of each other: $L_{eff} = PI(z_{max}) / \left(\frac{d\bar{PI}(z)}{dz} \right)$.

The lower figure shows the residuals between the phase integral and the fit function over the core part of the undulator magnet. A running wiggler-period-averaged function is plotted in black. The horizontal lines indicate the mean (center red line) and the rms deviations from the mean (two blue lines above and below the mean) of that wiggler-period-averaged function. The corresponding mean and rms values are also printed on the right hand side underneath the figure. On the lower left of the plot, the total phase integral accumulated along the undulator magnet, is shown, i.e., $PI(z_{max})$, the right-hand side value of the blue line in the upper plot.

The wiggler period averaged phase deviation, $\langle \Delta\phi \rangle_{\lambda_u}(z)$ can be calculated from $PI(z)$ via

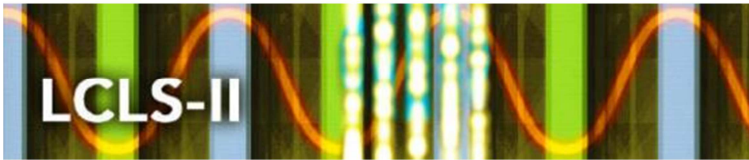
$$\langle \Delta\phi \rangle_{\lambda_u}(z) = \frac{2\pi}{L_{2\pi}} \left(\frac{e}{m c} \right)^2 \int_{z - \frac{\lambda_u}{2}}^{z + \frac{\lambda_u}{2}} (PI(\hat{z}) - \bar{PI}(\hat{z})) d\hat{z},$$

integrated over the undulator core.

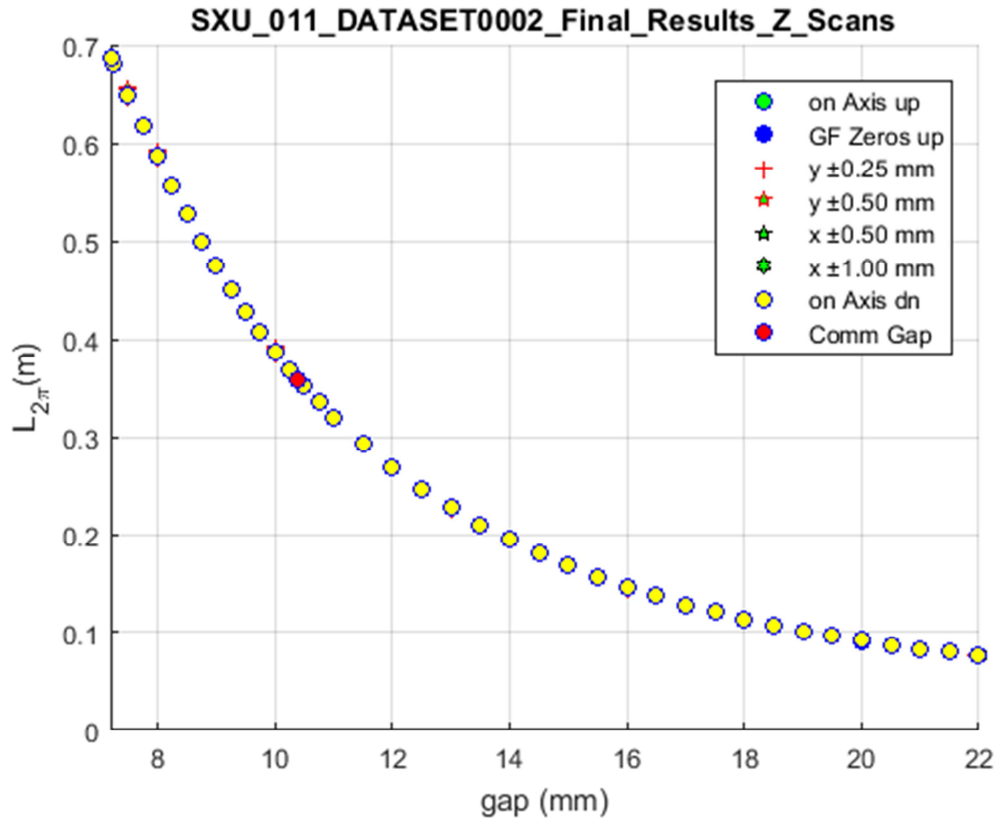
Here $L_{2\pi} = \lambda_u \left(1 + \frac{1}{2} K_{eff}^2 \right)$ (see next figure) is the free space distance over which a phase slippage of 2π occurs. The phase shake, $(\langle \Delta\phi \rangle)_{rms}$, which will be discussed later in this document is calculated as

$$(\langle \Delta\phi \rangle_{\lambda_u})_{rms} = \left(\langle \phi \rangle_{\lambda_u}(z) - \langle \langle \phi \rangle_{\lambda_u}(z) \rangle \right)_{rms}$$

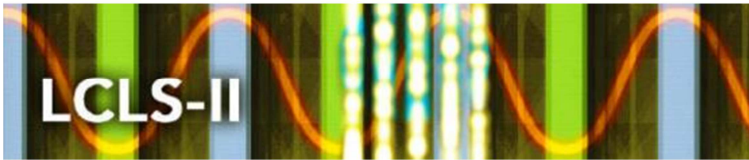
The following figures show the results of the gap dependent analysis.



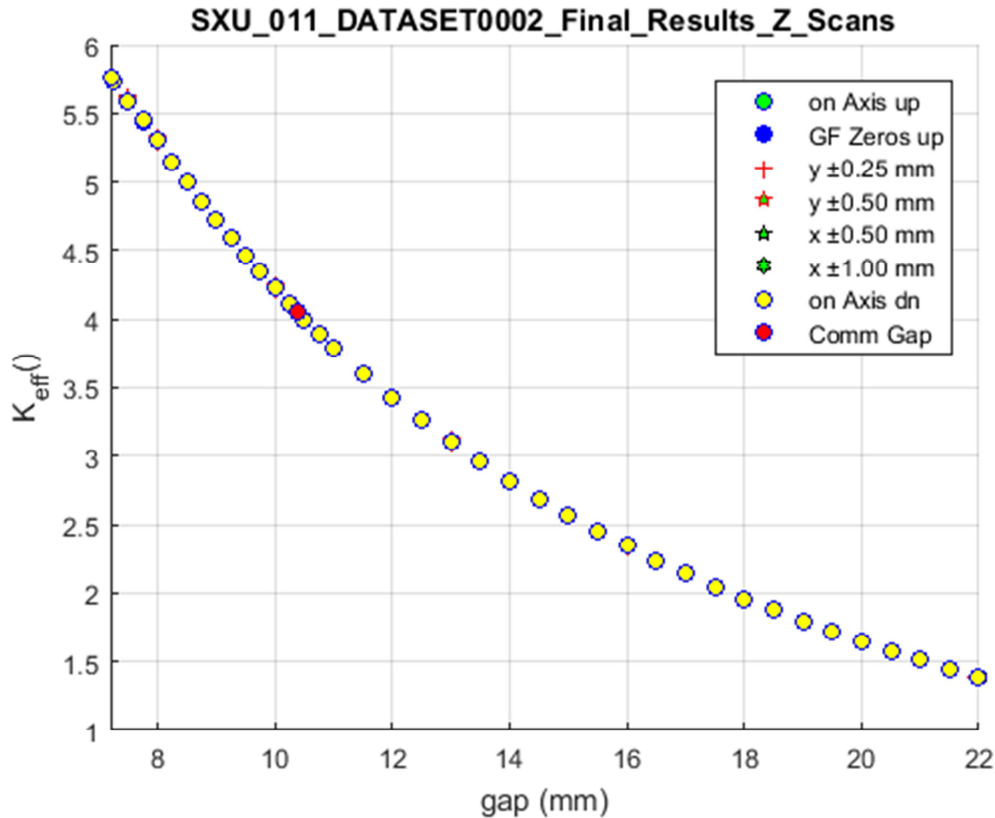
Evaluation of Hall Scans: $L_{2\pi}$ vs gap



The figure shows the free space distance over which a 2π slippage occurs between the radiation field and the electron bunch (see explanation above) as a function of undulator gap over the operational gap range. Note: the free space travel distance required to accumulate 2π slippage gets shorter towards larger gap values, which correspond to shorter undulator wavelengths. [Documentary Information]

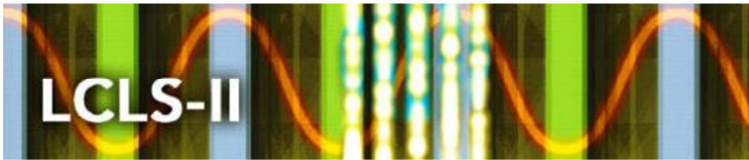


Evaluation of Hall Scans: K_{eff} vs gap

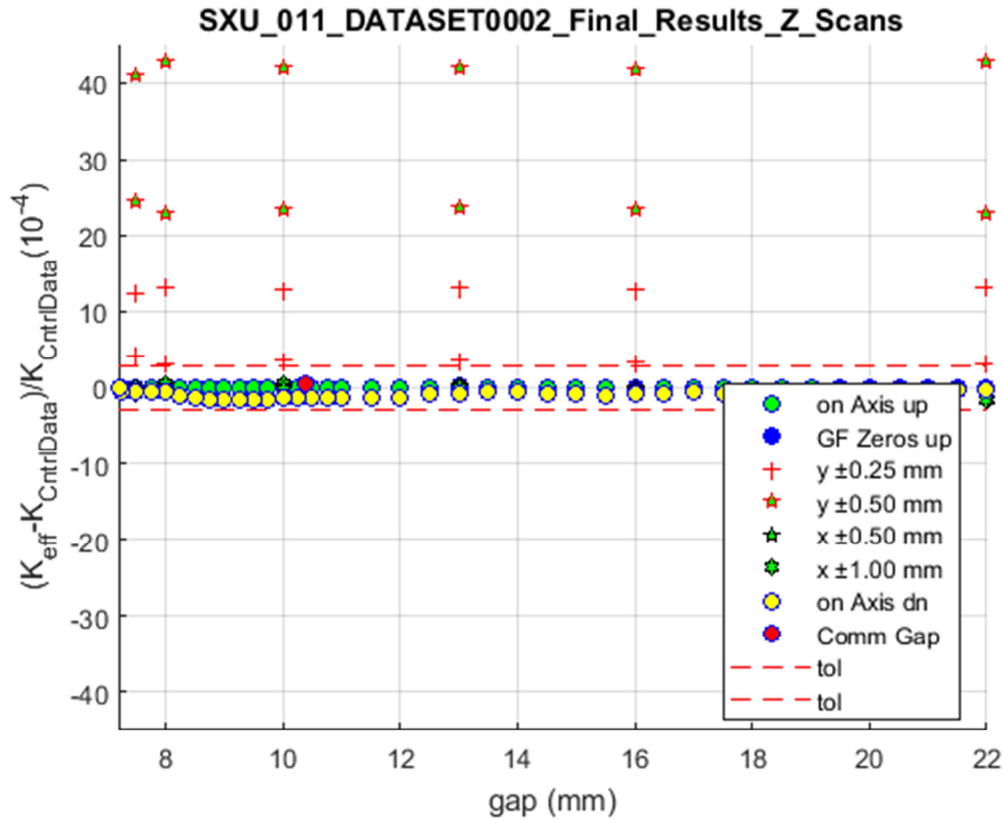


The figure shows undulator strength K_{eff} as a function of gap over the 7.2 mm – 22 mm operational range. The legend shows a number of different cases that will be explained later in this document because their effect cannot be observed in this full scale plot. Note: The gap values are derived from the readings of the two gap encoders installed on the SXU. In that sense these are nominal gap numbers that will be close but not identical to each of the individual pole separations measured across the undulator gap.

The continuous conversion between the two axes (i.e. $K_{eff}(gap)$ and $gap(K_{eff})$) will be done during operations based on the list of reference data points stored in file `sxu_011_k_vs_gap_spline.dat` in the Controls Data folder on the V: drive (see final section of this document for file information). From that list $K_{eff}(gap)$ and $gap(K_{eff})$ can be calculated via cubic spline fits or equivalent. [Documentary Information]

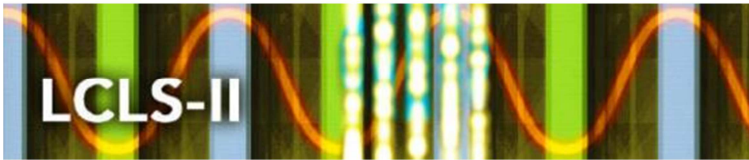


Evaluation of Hall Scans: $K_{eff} - K_{control}$ vs gap

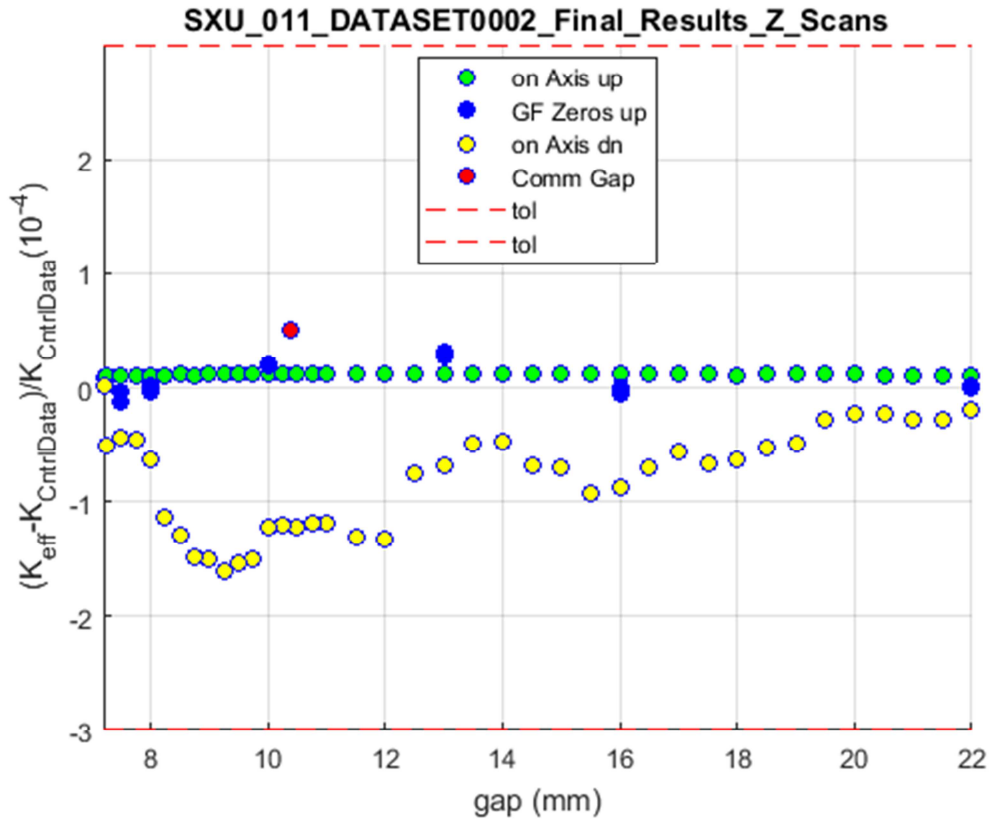


The figure shows the relative difference between the measured undulator strength K_{eff} and a cubic spline fit to the list of reference data points stored in file `sxu_011_k_vs_gap_spline.dat` in the Controls Data folder on the V: drive as a function of gap over the 7.2 mm – 22 mm operational range.

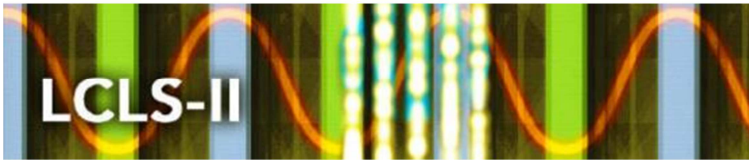
The legend explains the different cases that are shown in the plot: The green filled circles are data acquired on axis as the gap was changed from close to open. The yellow filled circles are data acquired on axis as the gap was changed from open to close. The horizontal red dashed lines show the tolerance limits. Note: The undulator K_{eff} value shows a hysteresis, i.e., for a given gap, the value depends on the direction of gap motion to reach that gap. While this is not a desirable feature, its effect stays within the given tolerance and will be acceptable. The other symbols shown indicate off-axis measurements that are added for interest only. The tolerance limits apply for on-axis readings, only



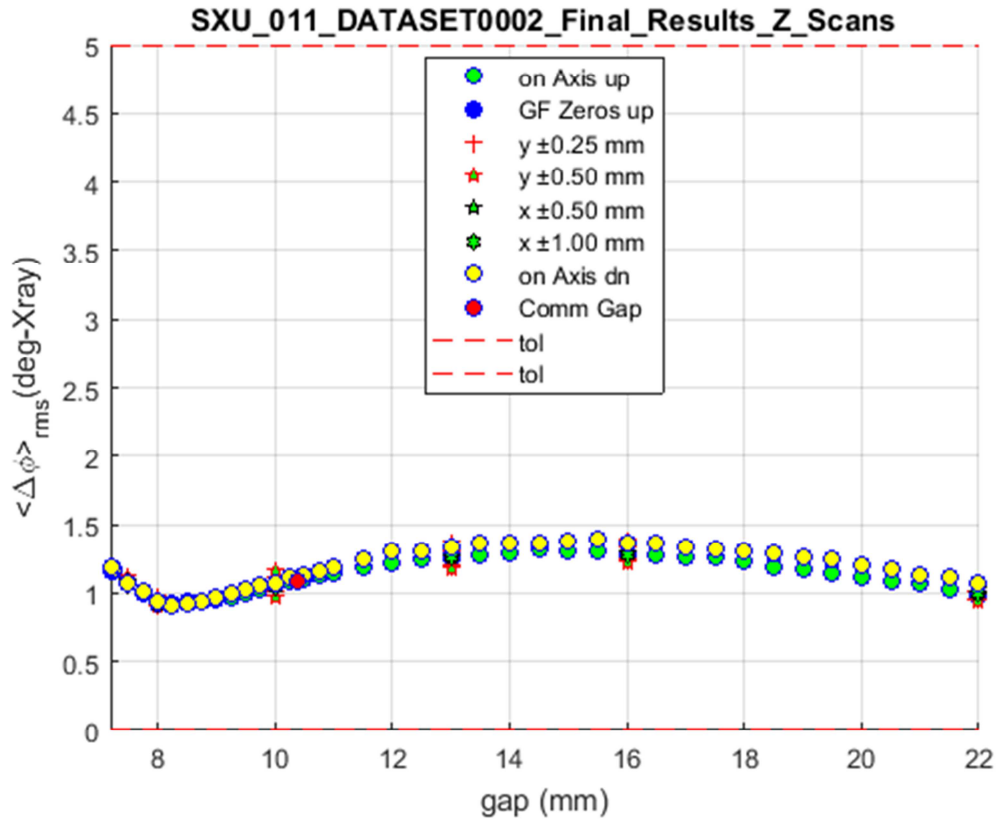
Evaluation of Hall Scans: $(K_{eff} - K_{CntrlData})/K_{CntrlData}$ vs *gap*



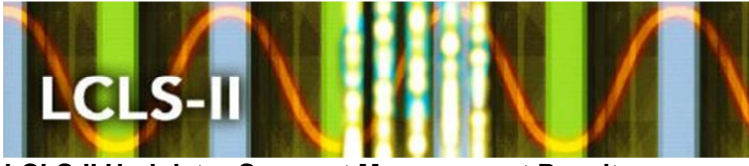
The figure shows some of the data shown in the previous figure but with a larger vertical scale that just captures the tolerance range. The hysteresis effect is more clearly visible. The off-axis measurements are not shown.



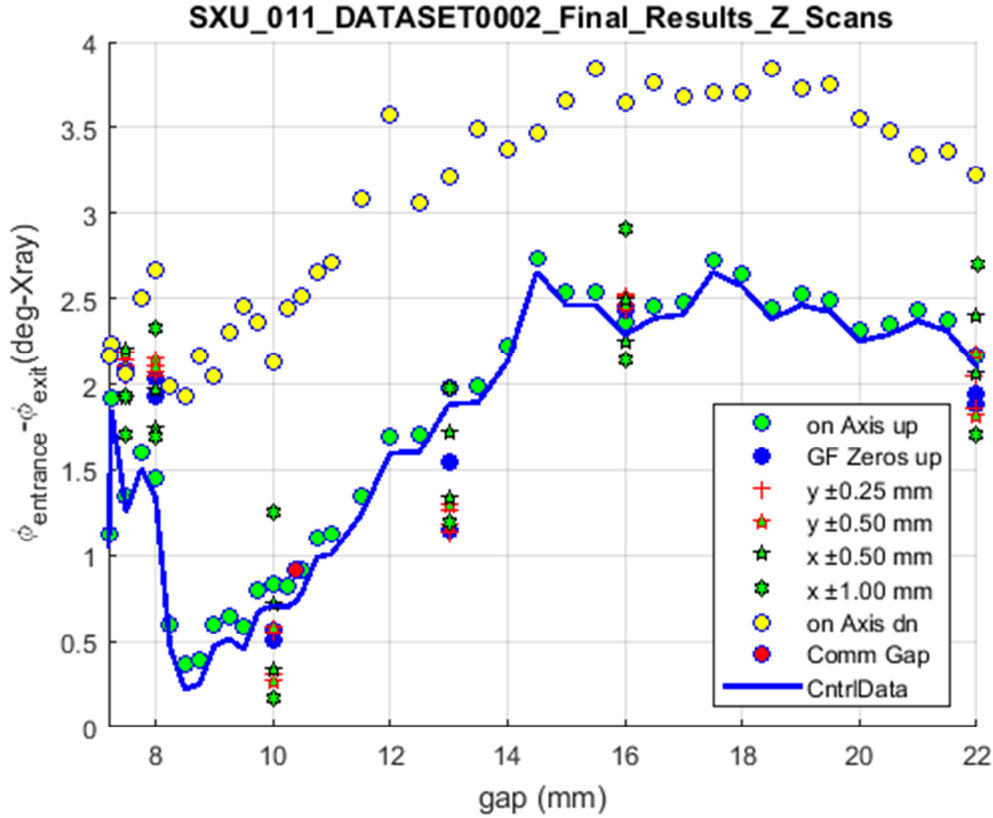
Evaluation of Hall Probe: Phase Shake vs. gap



The figure shows the phase shake, $\langle \Delta\phi \rangle_{rms}$, (see above) as a function of operational gap. The vertical axis extends over the entire tolerance range. The values show a slight hysteresis (show explanation above) but are well within tolerance.



Evaluation of Hall Probe: Entrance to Exit Phase Error Balance vs. gap



The figure shows a (negligible) imbalance of the entrance (cell boundary start to undulator core) to the exit (undulator core to cell boundary end) phase slippage for the undulator. In addition to the signals described above, the blue curve is a spline fit to the difference of the data in files

“..._phase_match_enter_vs_gap_spline.dat”

“..._phase_match_exit_vs_gap_spline.dat”.

The small change in phase difference between opening and closing measurements shows the effect of gap hysteresis. The explanation for the legend items can be found on previous pages above. The entrance and exit phase slippage is calculated as

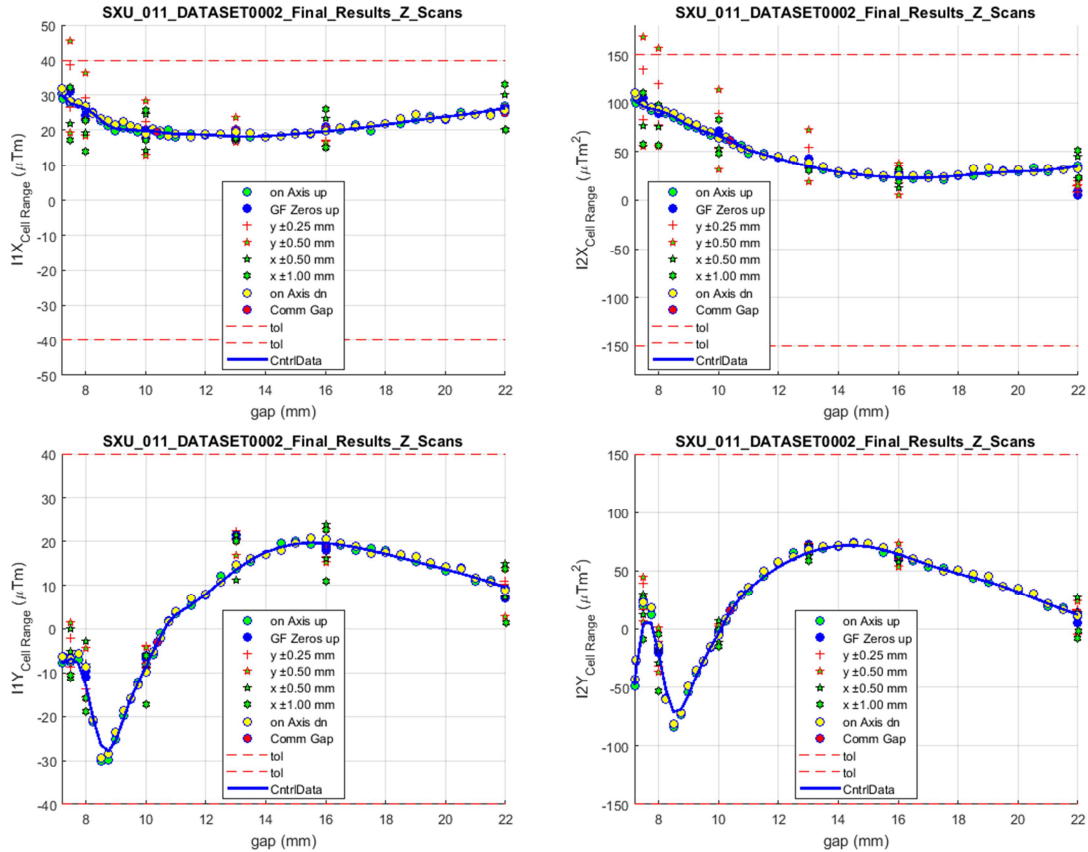
$$\phi_{entrance} = -\phi(z_{Cell-Start}) + \frac{1}{n+1} \sum_{j=1}^{n+1} (\phi(z_{B0,j}) - \pi(j-1)),$$

$$\phi_{exit} = \phi(z_{Cell-End}) - \frac{1}{n+1} \sum_{j=1}^{n+1} (\phi(z_{B0,j}) + \pi(n+1-j)).$$

Here, $z_{B0,j}$ is the z location of the zero crossing of $B_y(z)$ in front of the j^{th} core B_y peak. $z_{B0,(n+1)}$ is the z location of the field zero of $B_y(z)$ after the last core B_y peak.



Evaluation of Hall Probe: Field Integrals vs. gap



The figures show the field integrals ($I1X$, $I2X$, $I1Y$, $I2Y$) as function of the operational gap. The proximity of the green and yellow circles shows that the field integrals are not sensitive to the hysteresis in K as seen on a previous page. The blue curves are spline fits to the data in files

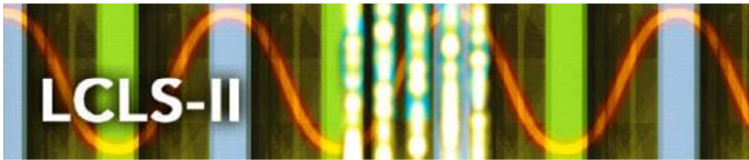
“...i1xvsgap_spline.dat”,

“...i2xvsgap_spline.dat”,

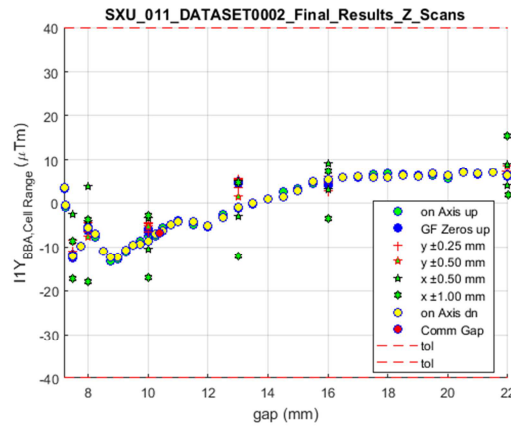
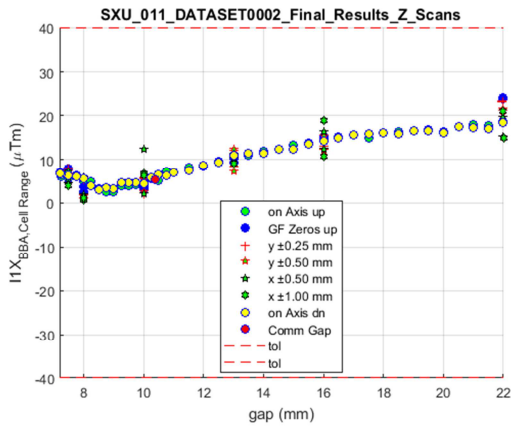
“...i1yvsgap_spline.dat”,

“...i2yvsgap_spline.dat”,

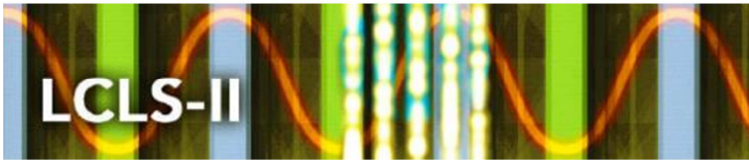
and demonstrate how the controls representations of the field integrals relates to the actual measurements (see final section of this document for file information).



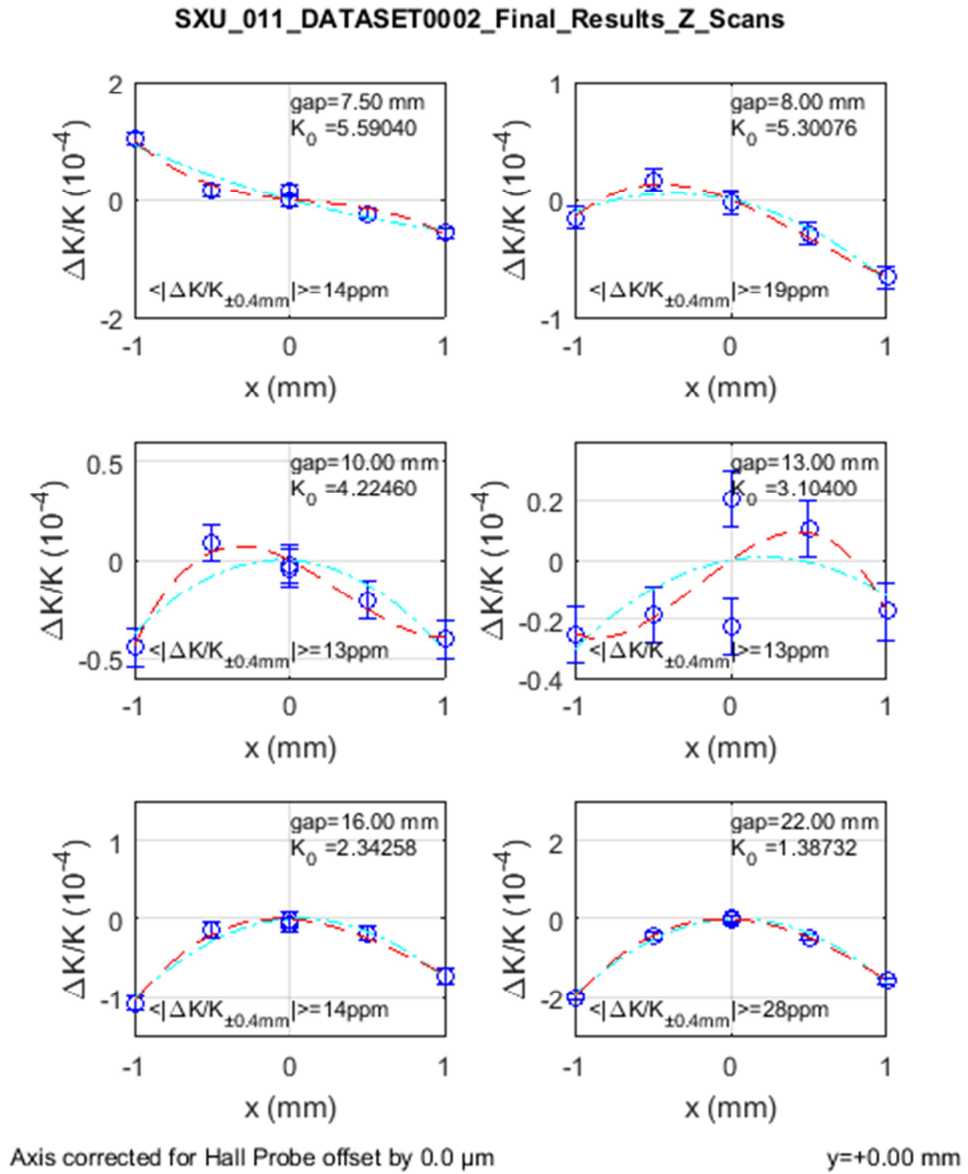
Evaluation of Hall Probe: BBA Corrected Field Integrals



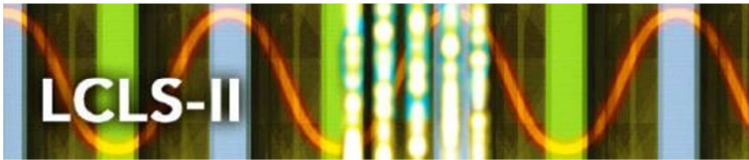
The figure shows the first integrals after a BBA equivalent correction was applied. The values stay within tolerance over the operational range.



Evaluation of Hall Probe: K vs. x dependence

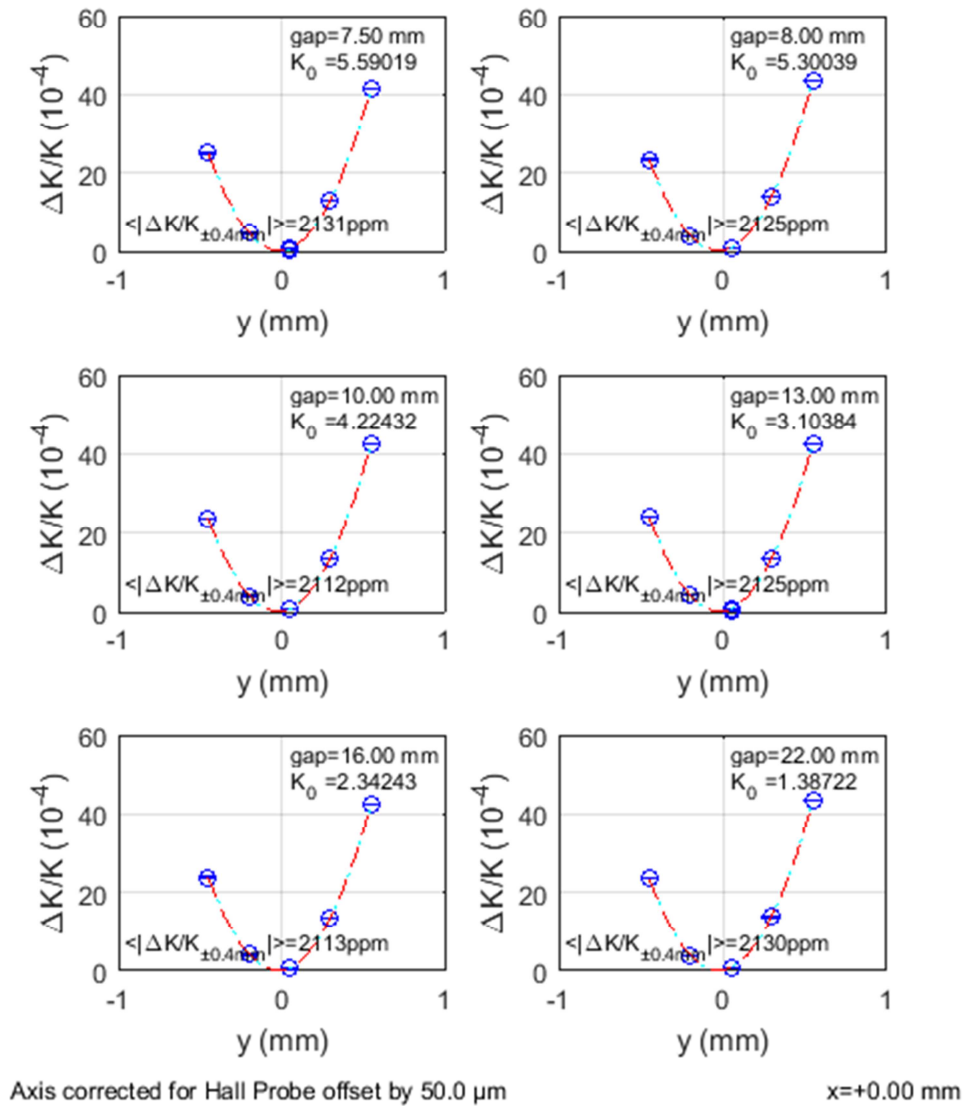


The figure shows the deviation of the relative undulator strength, K , from the off-axis value, K_0 , as function of x at a number of operational gaps. The average deviation at $z=0.4$ mm is well below the tolerance of 160 ppm in all cases.

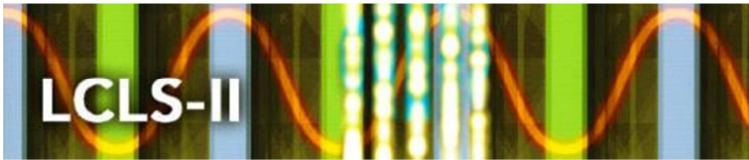


Evaluation of Hall Probe: K vs. y dependence

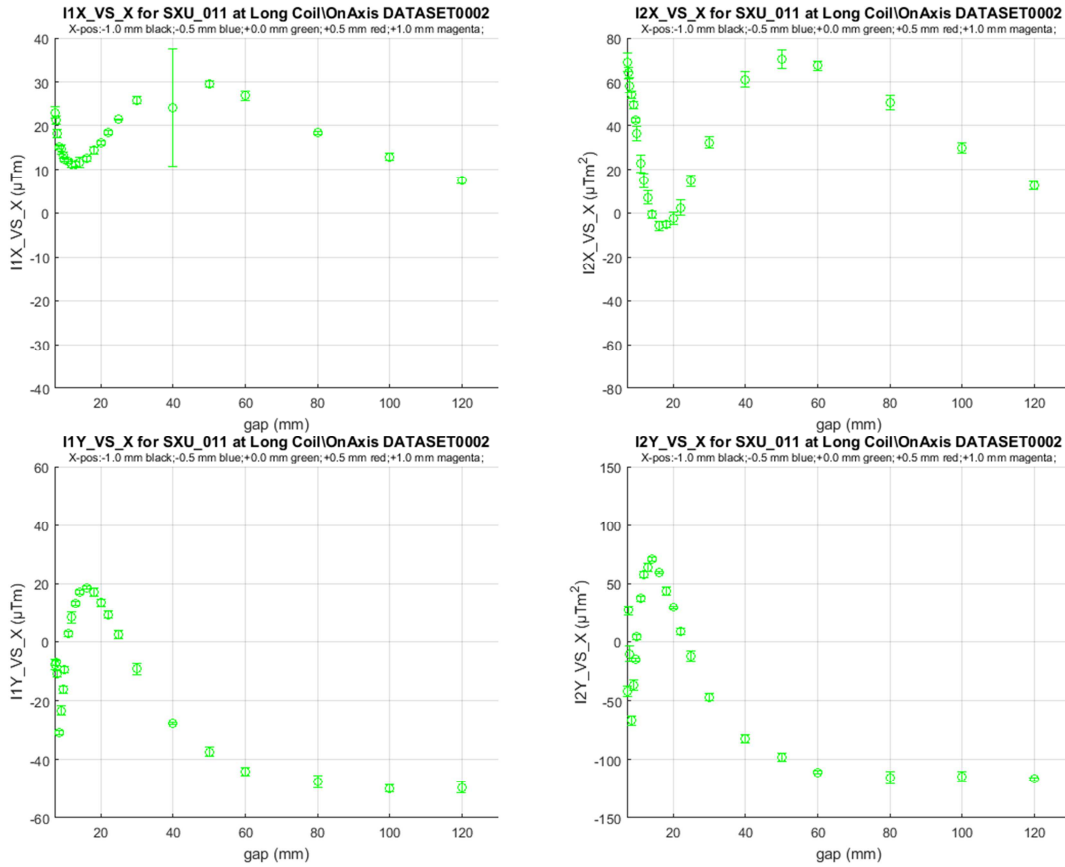
SXU_011_DATASET0002_Final_Results_Z_Scans



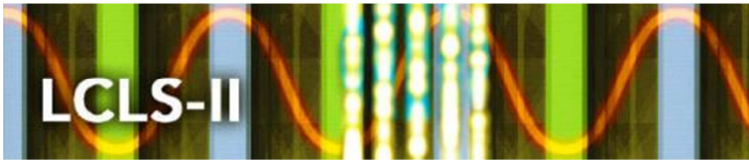
The figure shows the deviation of the relative undulator strength, K , value from the on-axis value, K_0 , as function of y at a number of operational gaps. The deviations follow closely the expected functional form $(\cosh(k_u y) - 1)$. [Documentary Information]



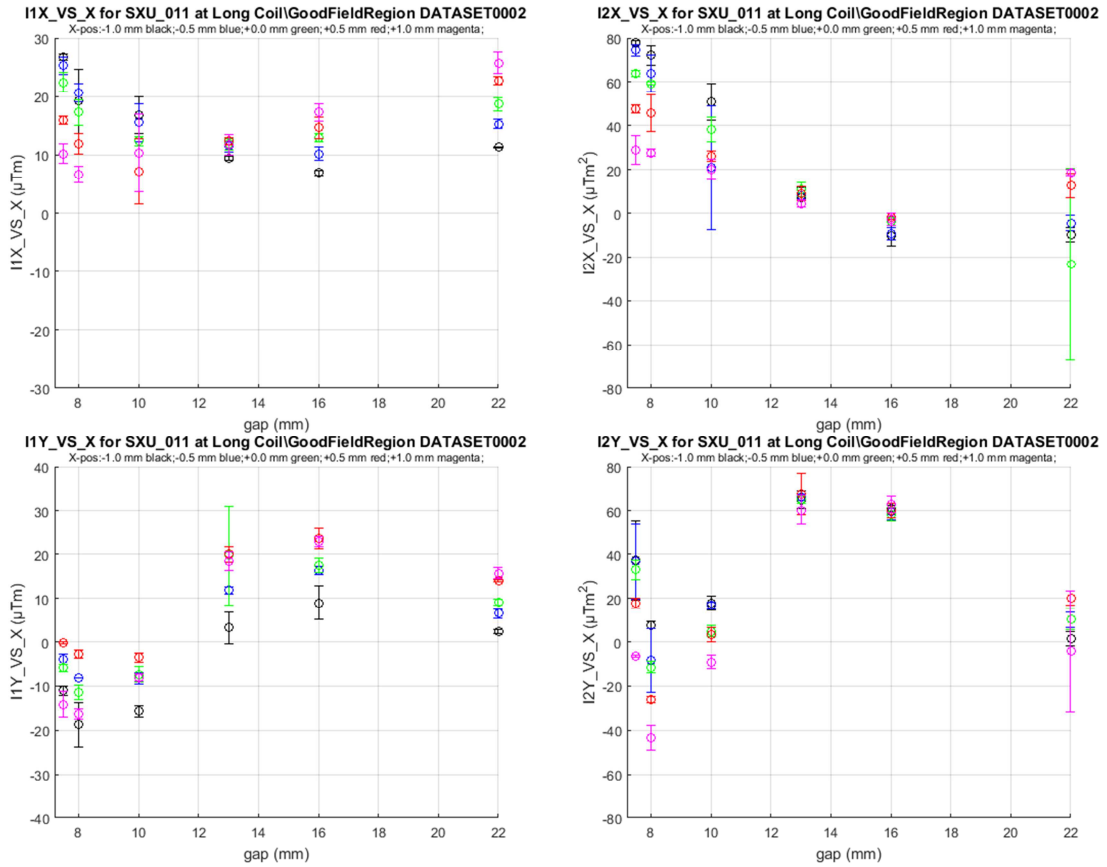
Long Coil Measurement of the On-Axis Field Integrals



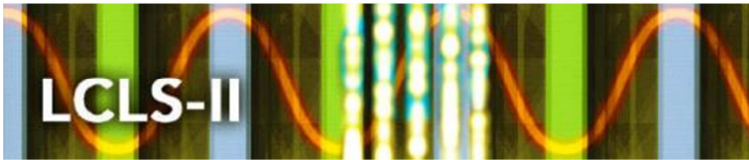
The figure shows the field integrals obtained from long coil measurements on-axis. The vertical axes extend over the tolerance range. All integrals are in tolerance.



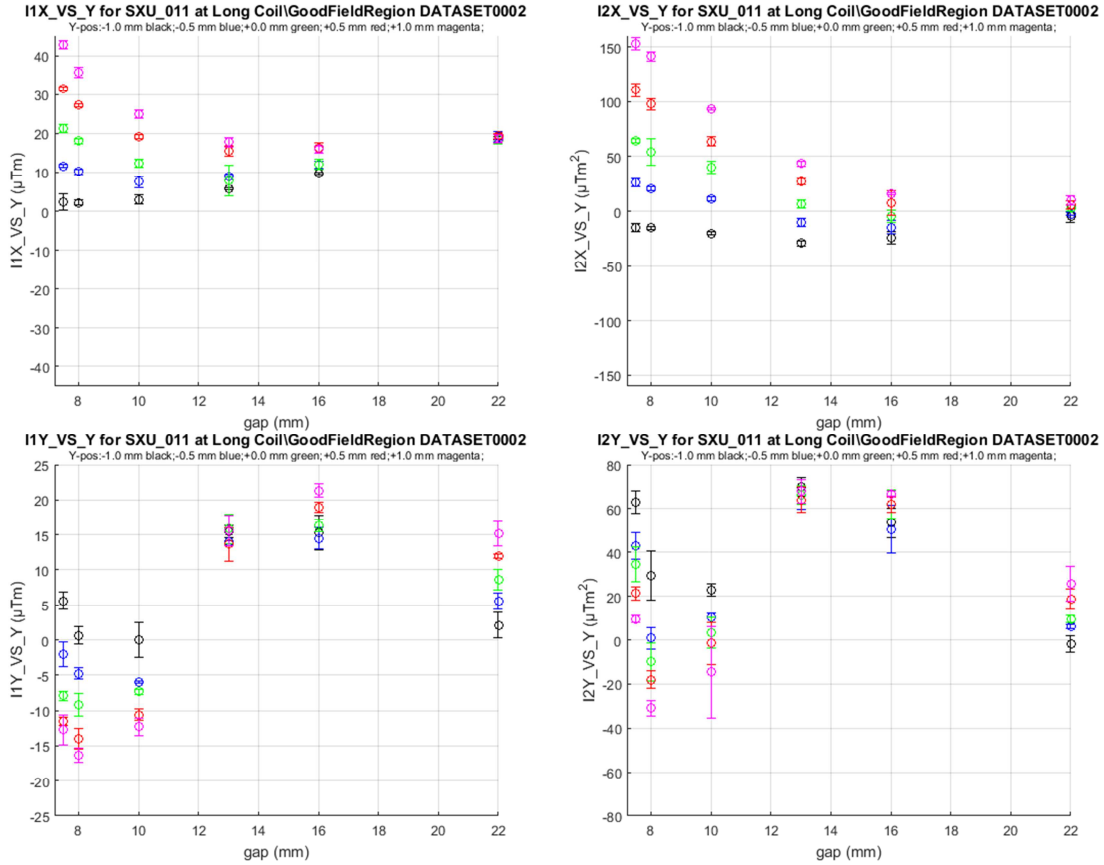
Long Coil Measurement of the Horizontally Off-Axis Field Integrals



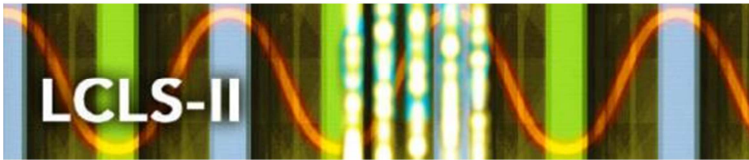
The figure shows the field integrals obtained from long coil measurements off axis in the horizontal plane using colors to indicate offset distance (black: -1.0 mm, blue: -0.5 mm, green: on-axis; red: +0.5 mm, magenta: +1.0 mm). The vertical axes extend over the tolerance range. All integrals are in tolerance.



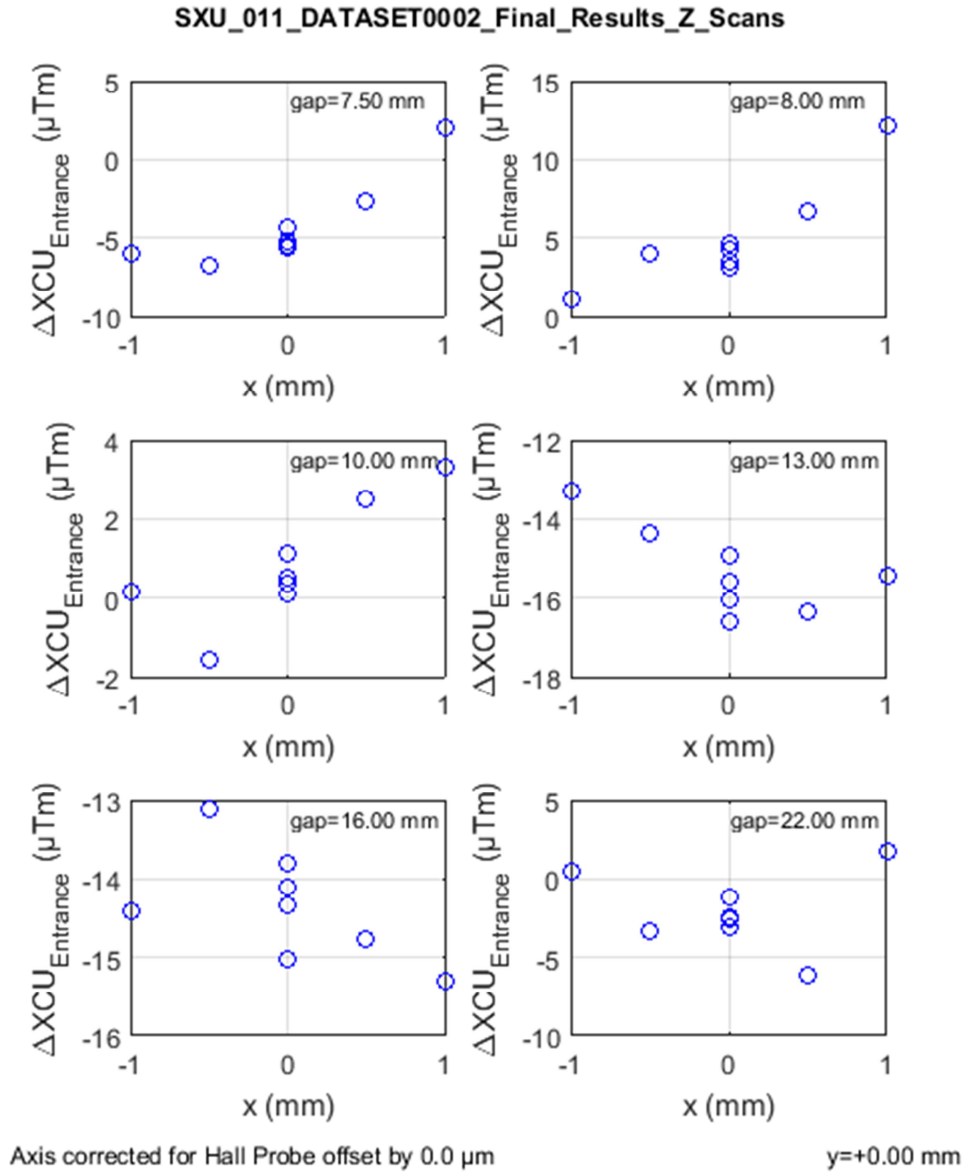
Long Coil Measurement of the Vertically Off-Axis Field Integrals



The figure shows the integrals obtained from long coil measurements off axis in the vertical plane using colors to indicate offset distance (black: -1.0 mm, blue: -0.5 mm, green: on-axis; red: +0.5 mm, magenta: +1.0 mm). The vertical axes extend of the tolerance range. All integrals are in tolerance.

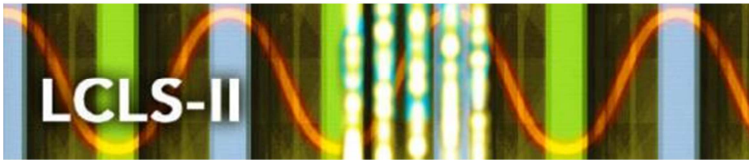


Estimated Upstream Horizontal Corrector Strength Requirement vs. x

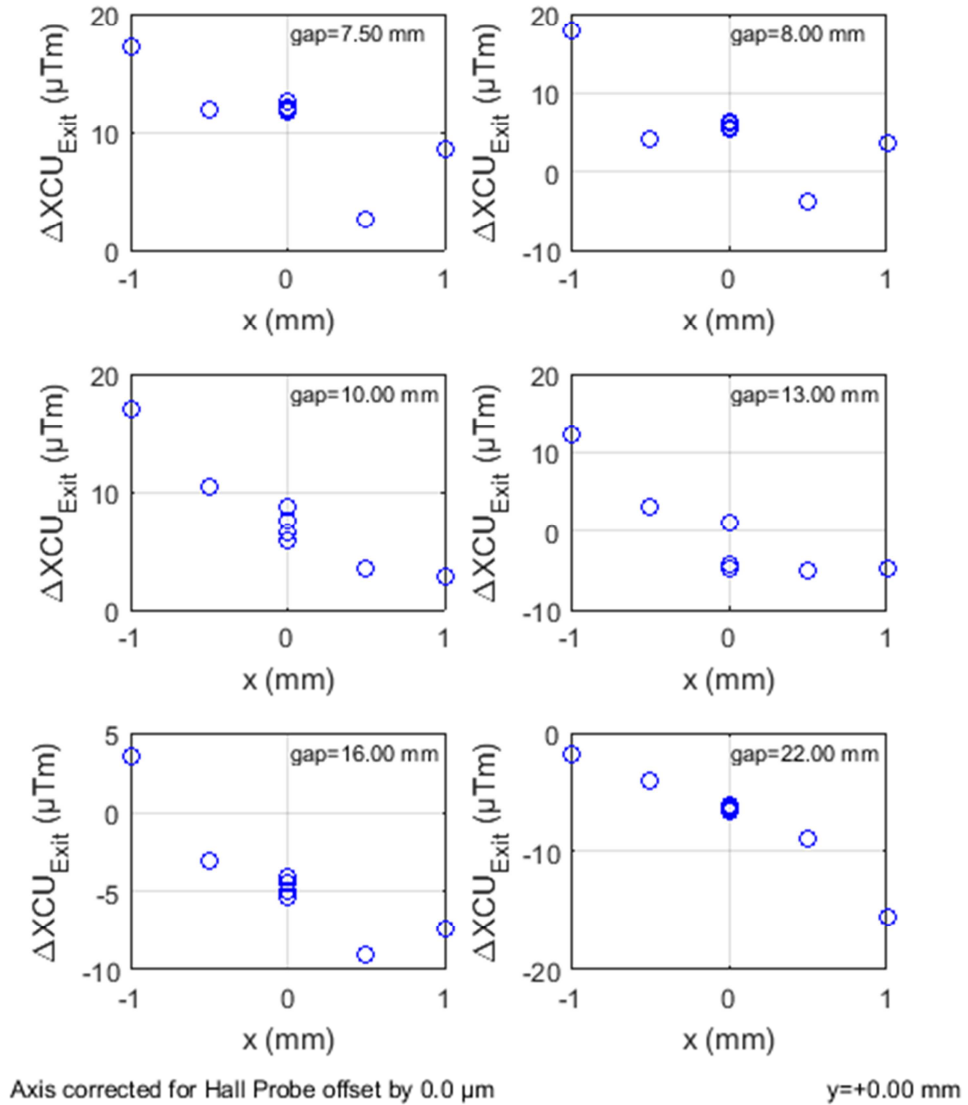


The figure shows the required strength of the upstream horizontal corrector to remove the second vertical undulator field integral at the downstream BPM for a number of operational undulator gaps. The analysis was done at a number of off-axis locations in the x-z plane. All values are small and well below the maximum correction capabilities of greater than 550 μTm of the actual correctors.

Estimated Downstream Horizontal Corrector Strength Requirement vs. x

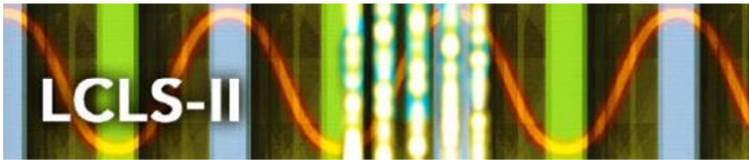


SXU_011_DATASET0002_Final_Results_Z_Scans

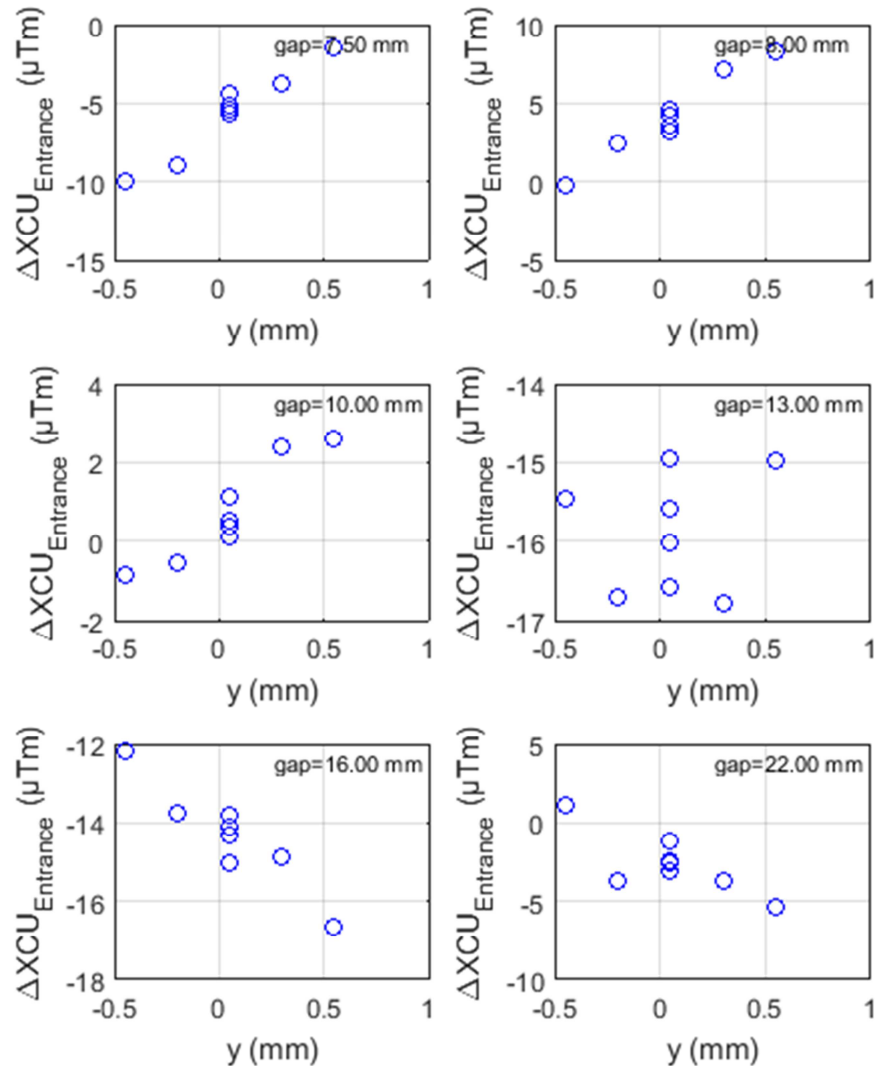


The figure shows the required strength of the downstream horizontal corrector to remove the first vertical undulator field integral and upstream corrector field integral at the downstream BPM for a number of operational undulator gaps. The analysis was done at a number of off-axis locations in the x-z plane. All values are small and well below the maximum correction capabilities of greater than 550 μTm of the actual correctors.

Estimated Upstream Horizontal Corrector Strength Requirement vs. y



SXU_011_DATASET0002_Final_Results_Z_Scans

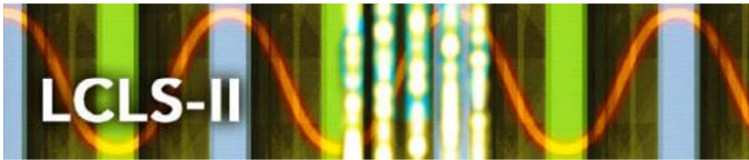


Axis corrected for Hall Probe offset by 50.0 μm

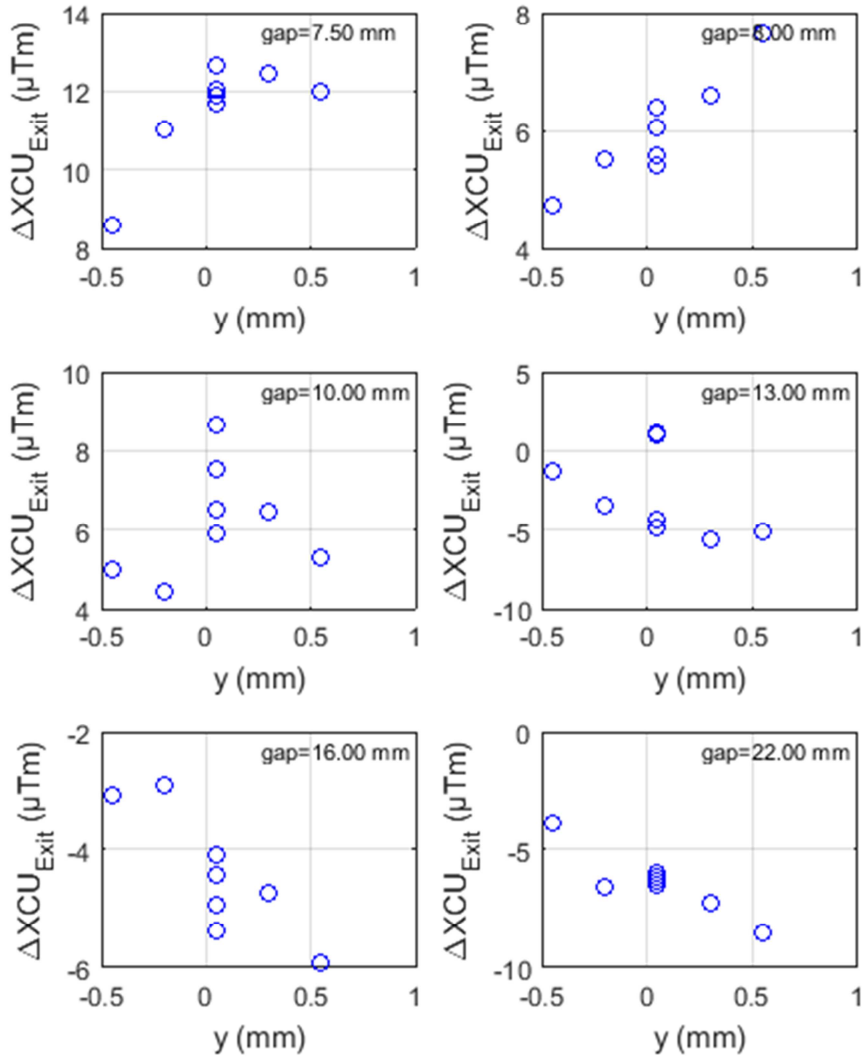
$x=+0.00$ mm

The figure shows the required strength of the upstream horizontal corrector to remove the second vertical undulator field integrals at the downstream BPM for a number of operational undulator gaps. The analysis was done at a number of off-axis locations in the y-z plane. All values are small and well below the maximum correction capabilities of greater than 550 μTm of the actual correctors.

Estimated Downstream Horizontal Corrector Strength Requirement vs. y



SXU_011_DATASET0002_Final_Results_Z_Scans



Axis corrected for Hall Probe offset by 50.0 μm

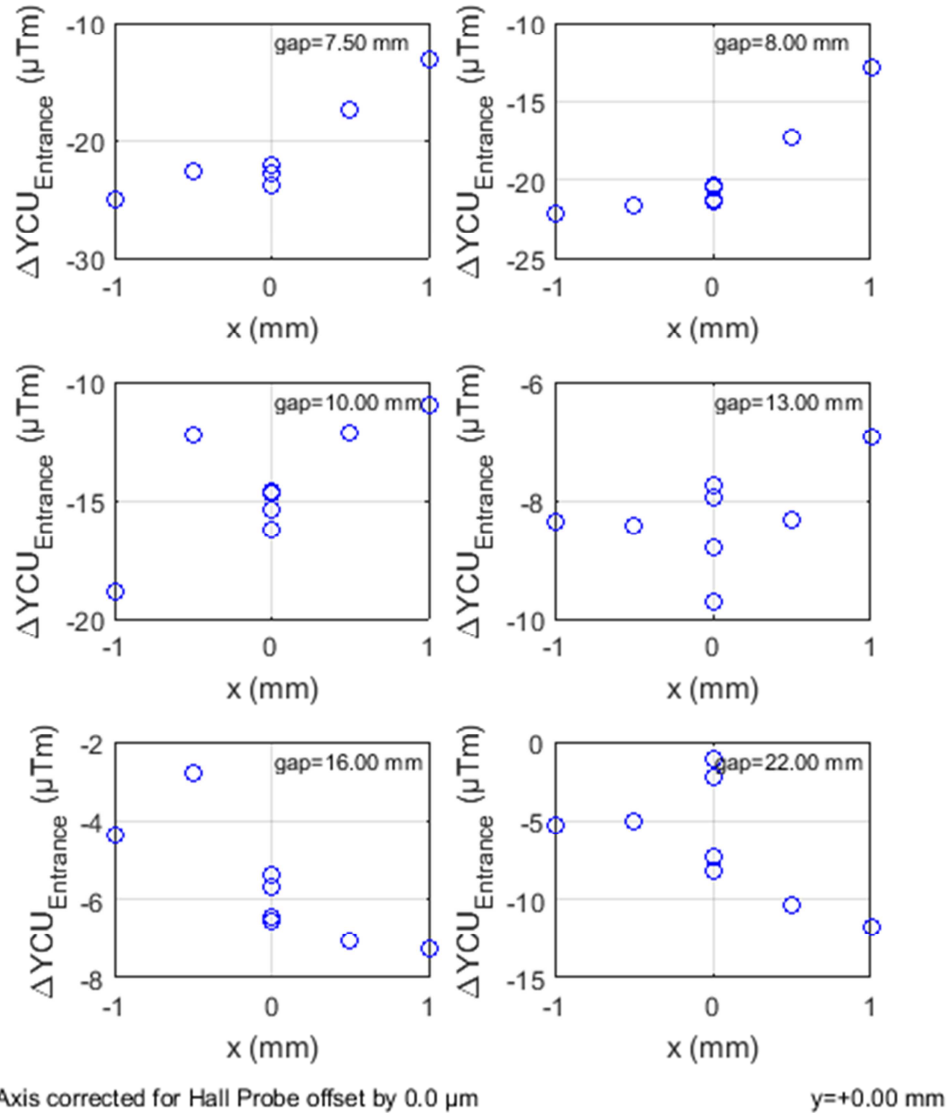
x=+0.00 mm

The figure shows the required strength of the upstream horizontal corrector to remove the first vertical undulator and upstream corrector field integrals at the downstream BPM for a number of operational undulator gaps. The analysis was done at a number of off-axis locations in the y-z plane. All values are small and well below the maximum correction amplitude of greater than 550 μTm capabilities of the actual correctors.

Estimated Upstream Vertical Corrector Strength Requirement vs. x

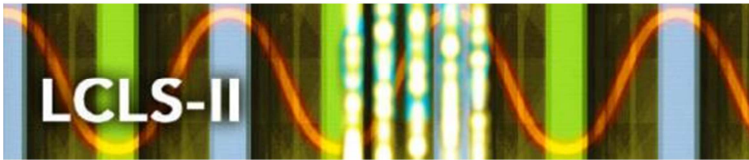


SXU_011_DATASET0002_Final_Results_Z_Scans

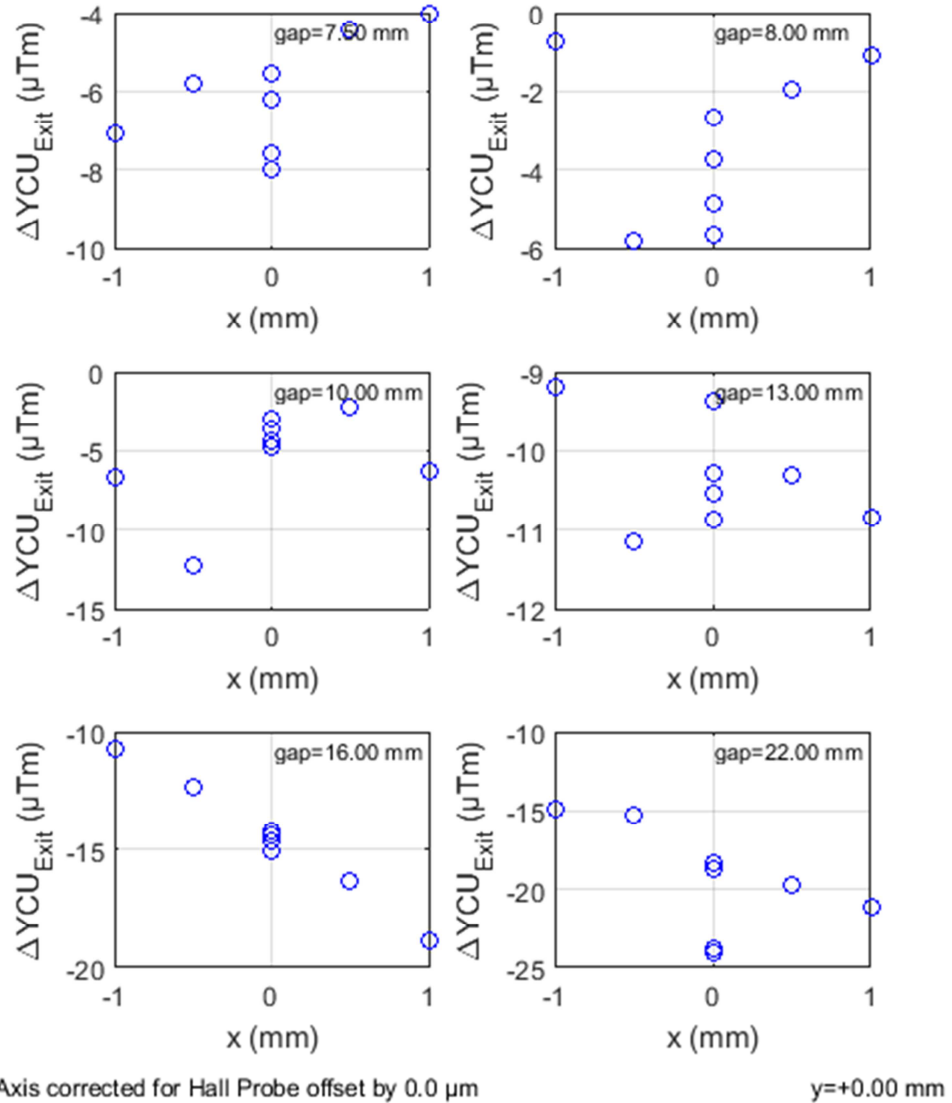


The figure shows the required strength of the upstream horizontal corrector to remove the second horizontal undulator field integral at the downstream BPM for a number of operational undulator gaps. The analysis was done at a number of off-axis locations in the x-z plane. All values are small and well below the maximum correction capabilities of greater than 550 μTm of the actual correctors.

Estimated Downstream Vertical Corrector Strength Requirement vs. x

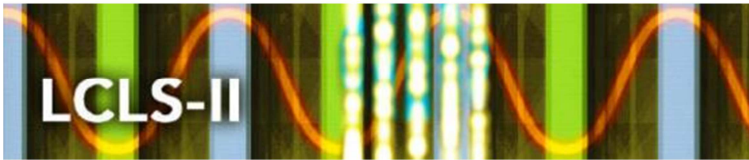


SXU_011_DATASET0002_Final_Results_Z_Scans

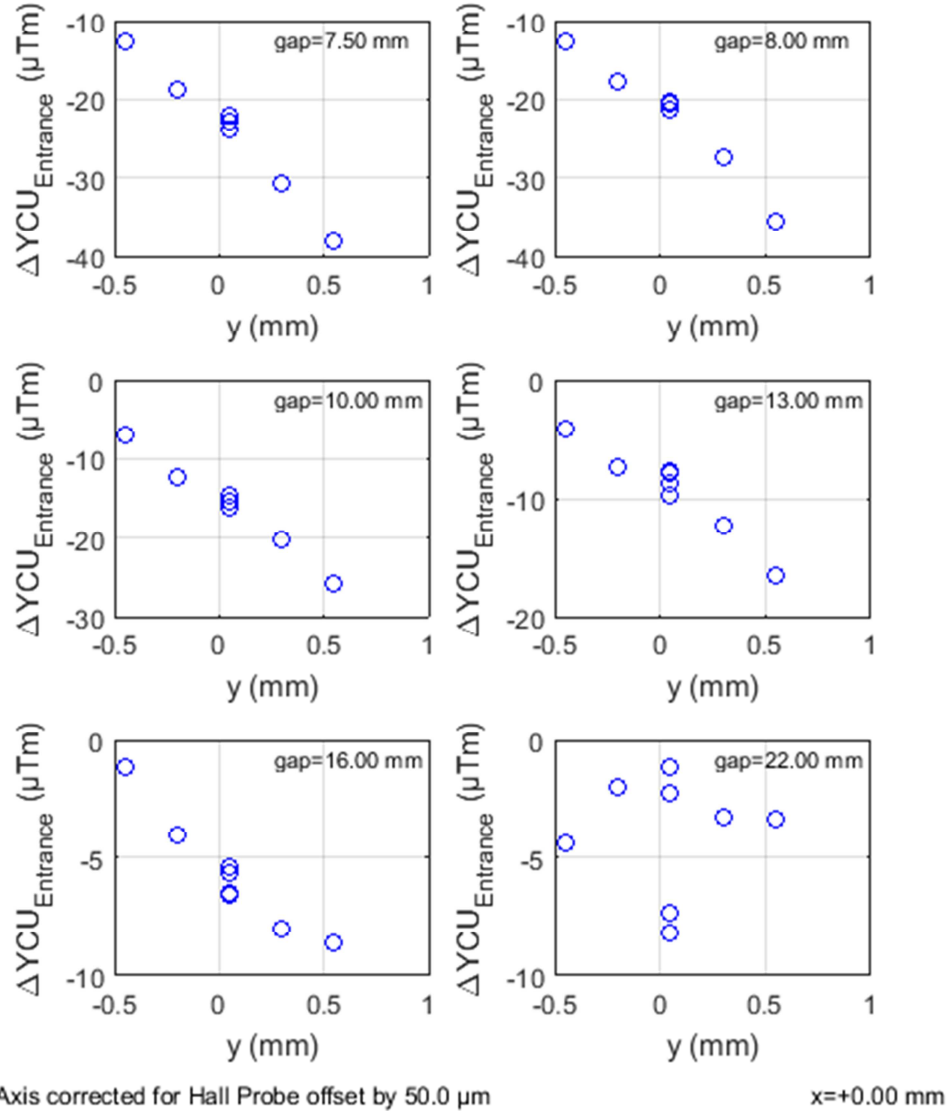


The figure shows the required strength of the downstream vertical corrector to remove the first horizontal undulator field integral and upstream corrector field integral at the downstream BPM for a number of operational undulator gaps. The analysis was done at a number of off-axis locations in the x-z plane. All values are small and well below the maximum correction capabilities of greater than 550 μTm of the actual correctors.

Estimated Upstream Vertical Corrector Strength Requirement vs. y

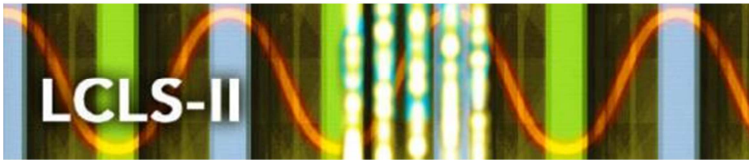


SXU_011_DATASET0002_Final_Results_Z_Scans

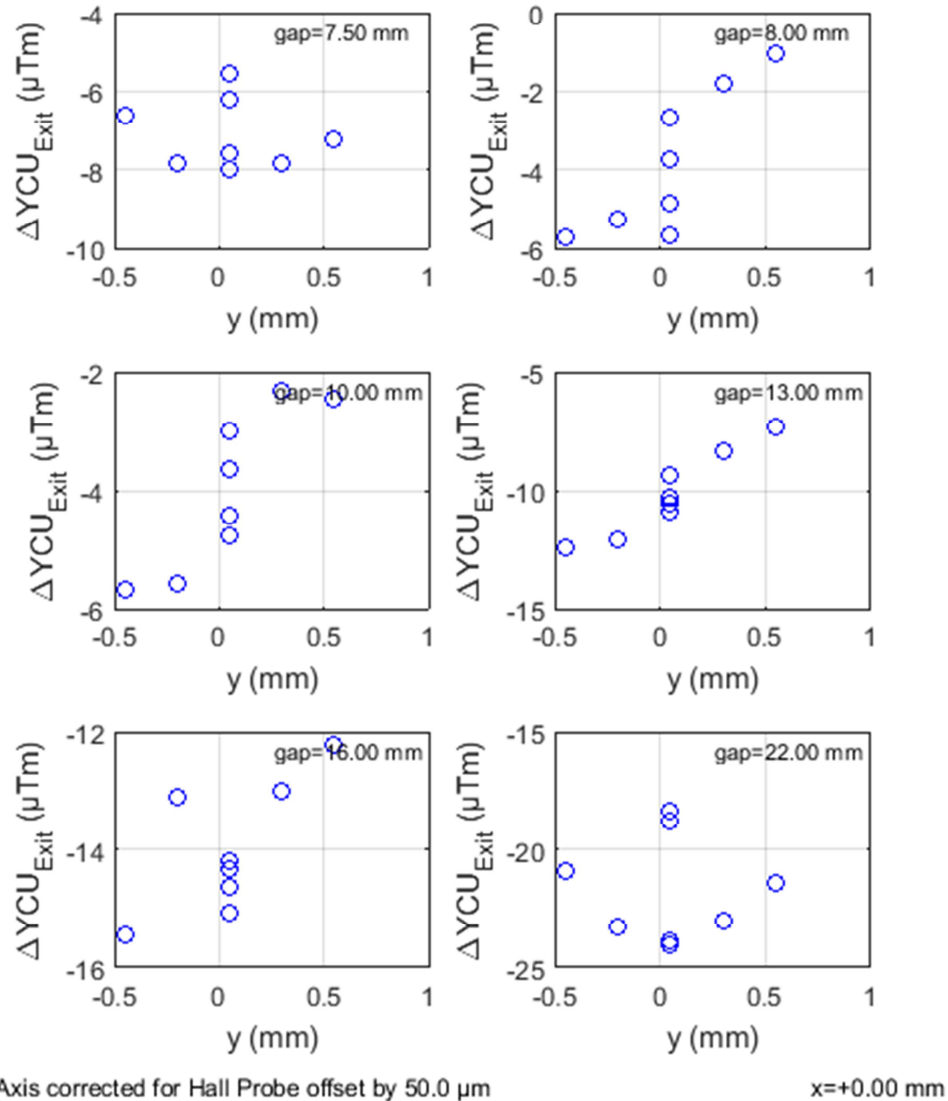


The figure shows the required strength of the upstream vertical corrector to remove the second horizontal undulator field integral at the downstream BPM for a number of operational undulator gaps. The analysis was done at a number of off-axis locations in the y-z plane. All values are small and well below the maximum correction capabilities of greater than 550 μTm of the actual correctors.

Estimated Downstream Vertical Corrector Strength Requirement vs. y



SXU_011_DATASET0002_Final_Results_Z_Scans



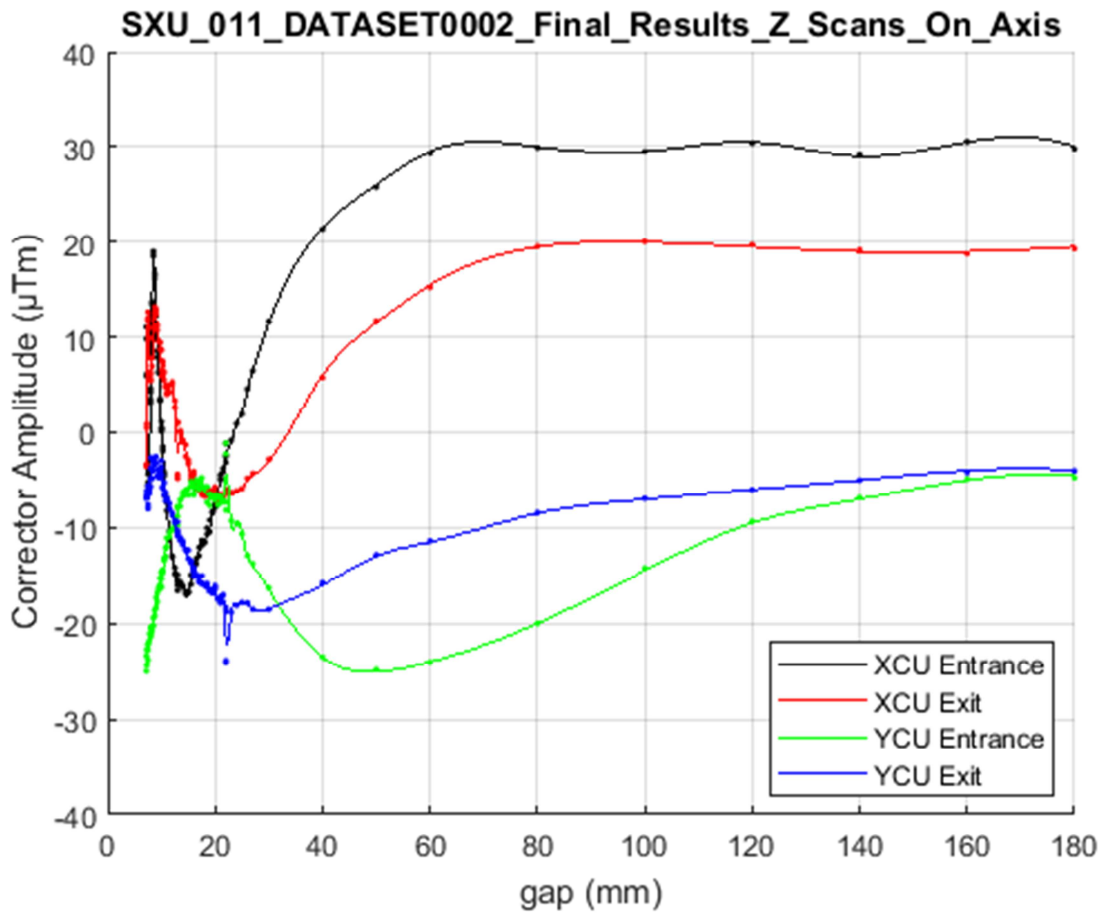
The figure shows the required strength of the downstream vertical corrector to remove the first horizontal undulator field integral and the upstream corrector field integral at the downstream BPM for a number of operational undulator gaps. The analysis was done at a number of off-axis locations in the y-z plane. All values are small and well below the maximum correction capabilities of greater than 550 μTm of the actual correctors.

Estimated Corrector Strengths Requirement vs. gap

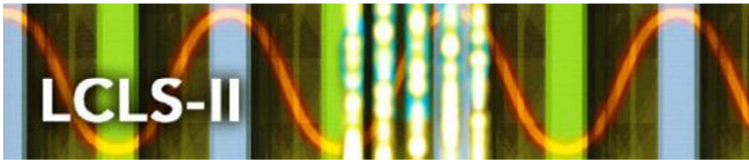


LCLS-II Undulator Segment Measurement Results

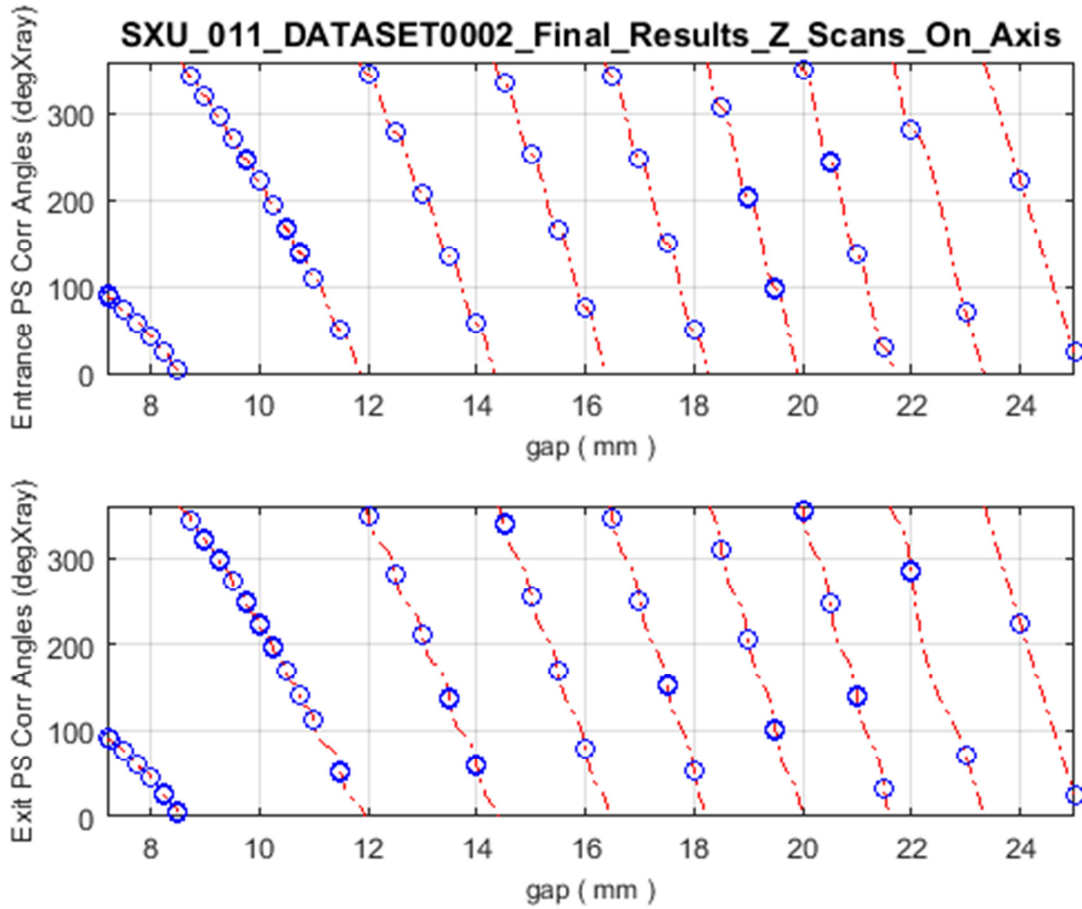
SXU-011



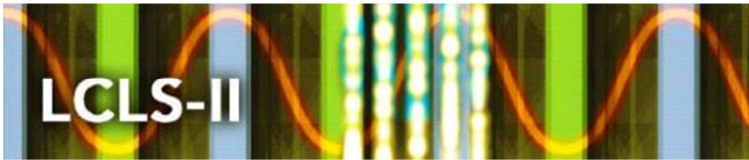
The figure shows as a function of undulator gap the required strengths of the upstream and downstream horizontal and vertical correctors to remove the effect of undulator field integrals at the downstream BPM over the entire available gap range. All values are small and well below the maximum correction capabilities of greater than 550 μTm of the actual correctors.



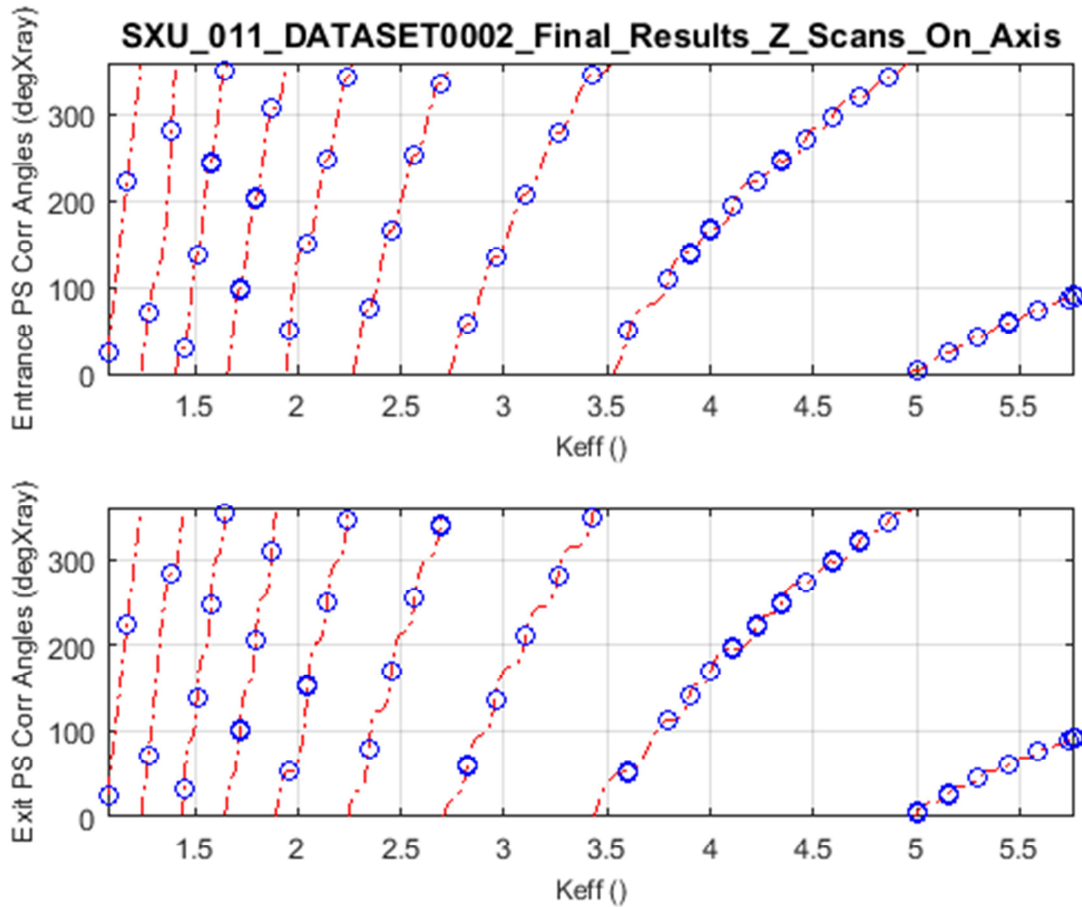
Estimated Phase Shifter (Angle) Change Requirement vs. gap



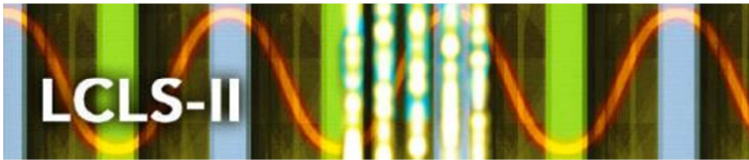
The top and bottom figures show as a function of undulator gap the required correction angles to be added to the upstream and downstream phase shifters, respectively. The red lines indicate the minimum required phase shifter phase angle increases, which are in the 0 to 360 degXray phase shift range. The blue circles indicate MMF measurements.



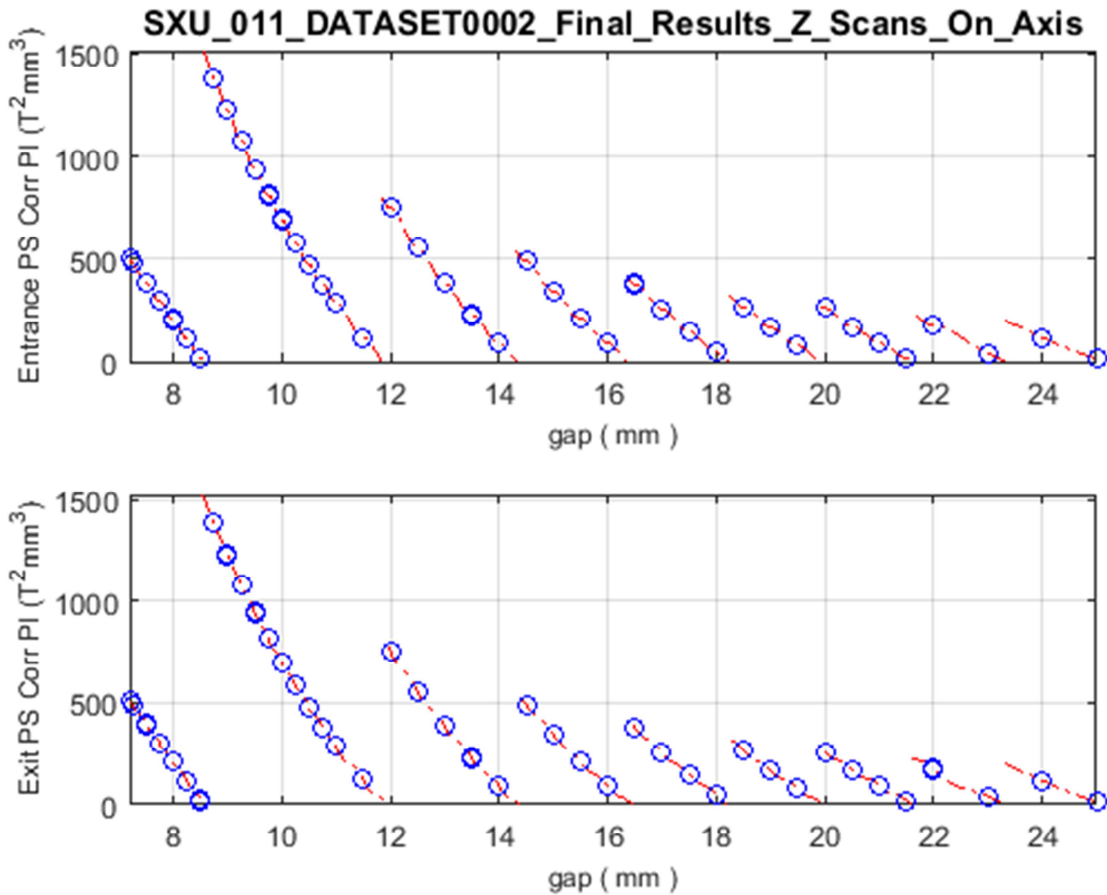
Estimated Phase Shifter (Angle) Change Requirement vs. K_{eff}



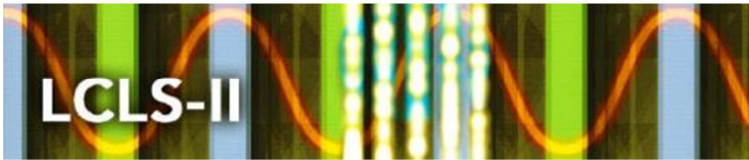
The top and bottom figures as a function of undulator parameter K_{eff} the required correction angles to be added to the upstream and downstream phase shifters, respectively. The red lines indicate the minimum required phase shifter phase angle increases, which are in the 0 to 360 degXray phase shift range. The blue circles indicate MMF measurements.



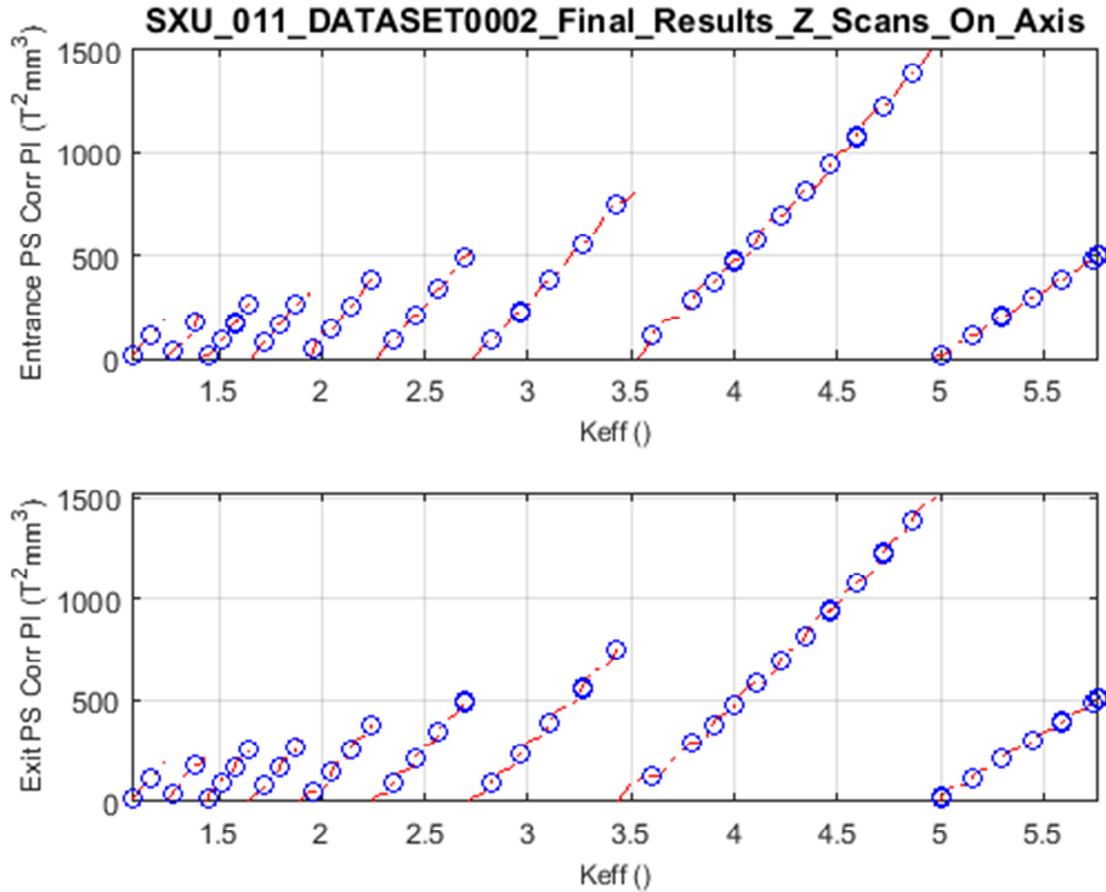
Estimated Phase Shifter (Phase Integral Change) Requirement vs. gap



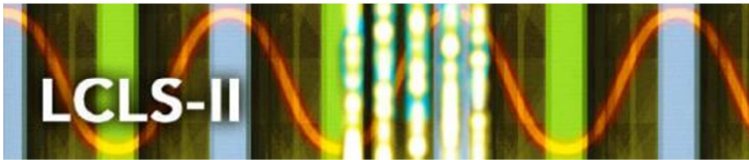
The top and bottom figures show as a function of undulator gap the required correction phase integral (PI) values to be added to the upstream and downstream phase shifters, respectively. The red lines indicate the minimum required phase shifter phase angle increases, which are in the 0 to 360 degXray phase shift range. The blue circles indicate MMF measurements.



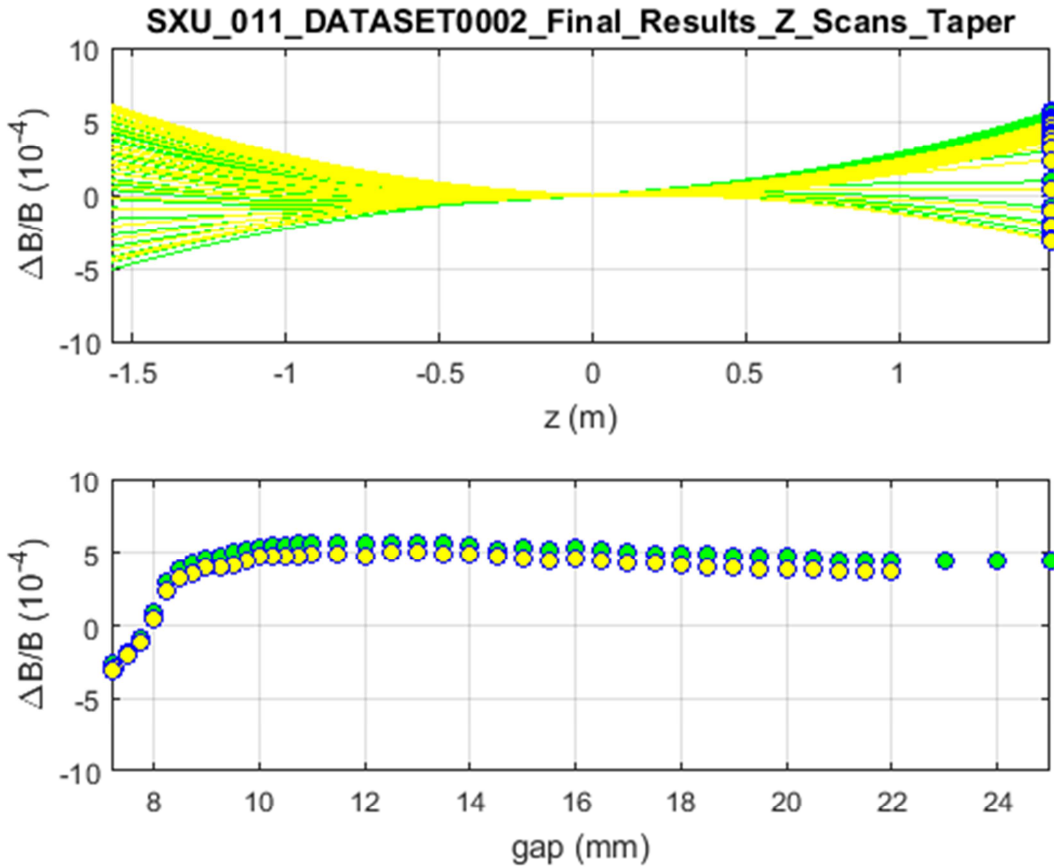
Estimated Phase Shifter (Angle) Requirement vs. gap



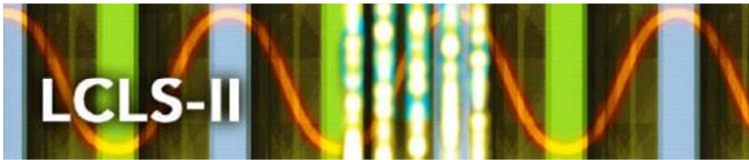
The top and bottom figures show as a function of undulator parameter K_{eff} the required correction phase integral (PI) values to be added to the upstream and downstream phase shifters, respectively. The red lines indicate the minimum required phase shifter phase angle increases, which are in the 0 to 360 degXray phase shift range. The blue circles indicate MMF measurements.



Zero Taper Fits vs. gap

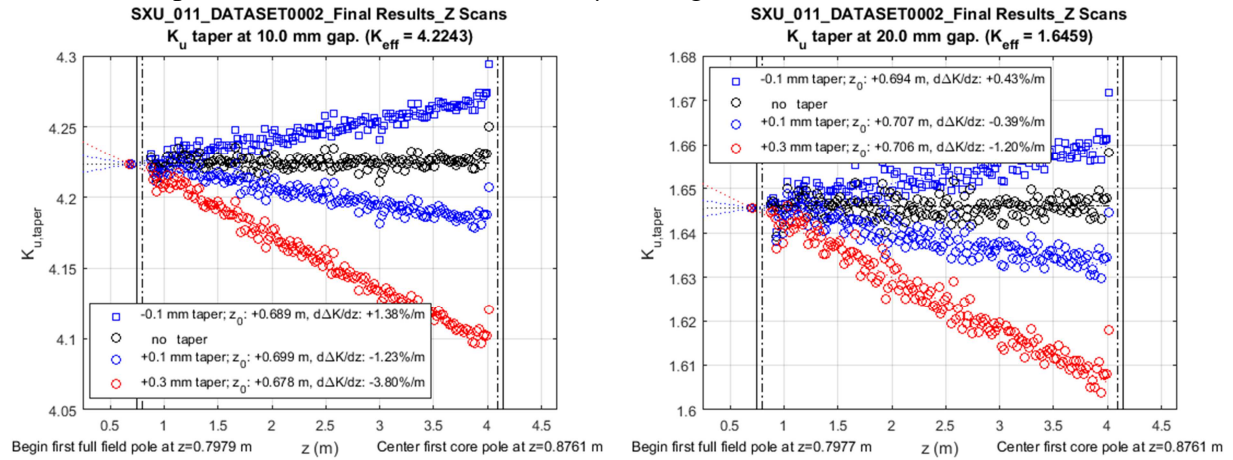


The top figure shows quadratic fits to the absolute values K_u for each core pole for different gaps when the device is set to zero taper. Green curves indicate that the gap was approached from smaller gaps, while yellow curves indicate approach from larger gaps. The fitted K_u value of the last pole is marked with a solid circle with the same color coding. The bottom shows the same solid circles as in the upper plot but this time plotted against the corresponding undulator gap encoder values. The figures show that the undulator has a small quadratic taper that varies with gap. This could explain the phase shake dependence on gap as shown in an earlier figure.



Gap Tapering – Tapered K_u values

The SXU devices support a gap taper, which is controlled by the taper PV, which holds the difference between the upstream and downstream gap encoder readings measured in micrometer. The taper can be varied over the $\pm 300 \mu\text{m}$ -range.



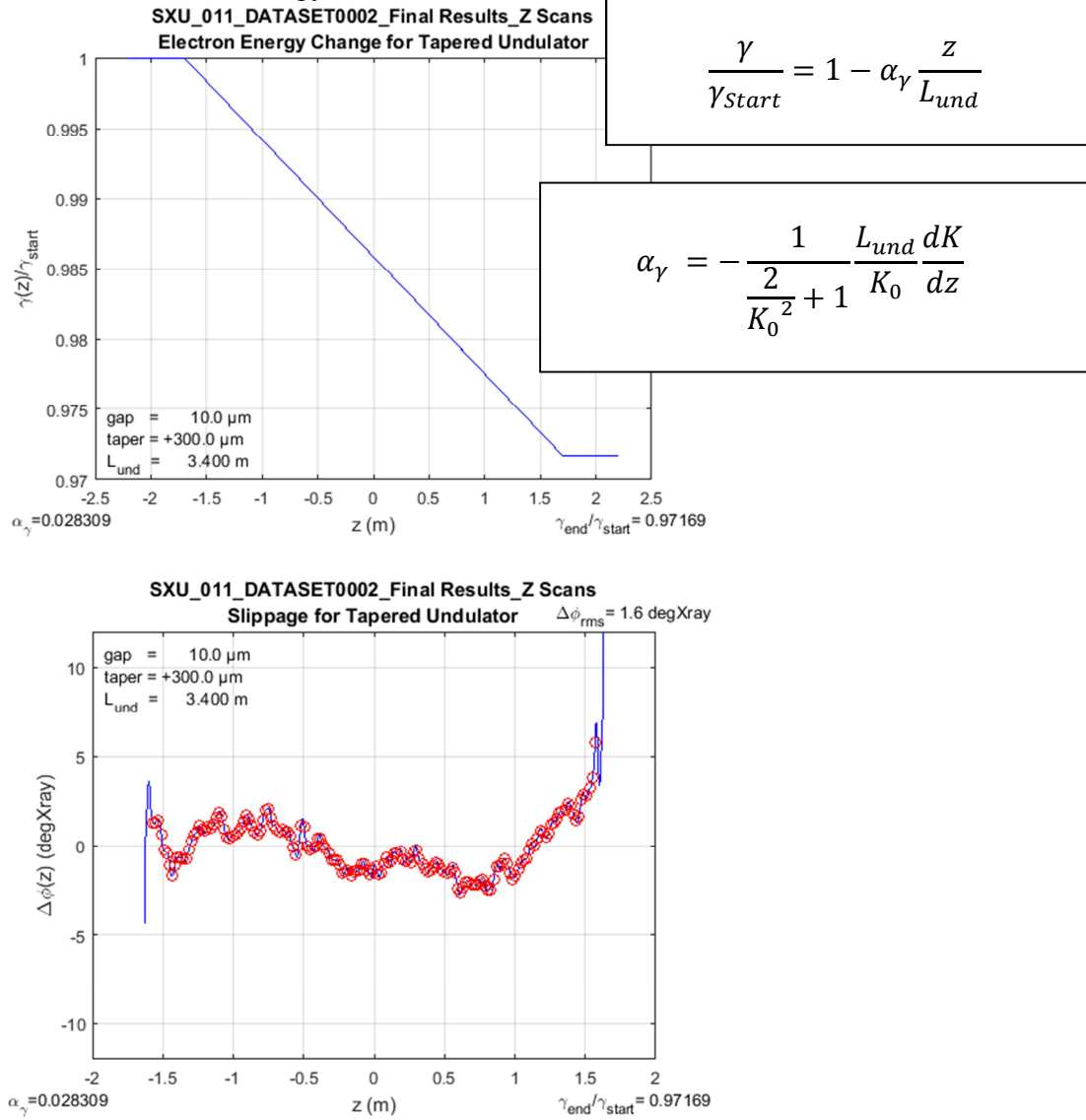
The figure shows $K_{u,taper}$ for the 162 core poles based on Hall probe measurements versus z location for 4 different taper amplitudes ($-100 \mu\text{m}$, $0 \mu\text{m}$, $+100 \mu\text{m}$, $+300 \mu\text{m}$) and 2 different gaps (8 mm, 20 mm). The vertical dashed lines indicate the beginning of the first and the end of the last full field pole. The solid vertical lines indicate the longitudinal limits of strongback. The crosses on the left hand side of the undulator segment border surrounded by the $K_{u,taper}$ symbol for the representative taper amplitude indicate the intersections between linear fits (indicated by dotted lines in the representative color) and the K_u values untapered case with each of the tapered cases. The horizontal dash-dotted line next to the figure center (hard to see) indicated the level of K_{eff} of the untapered undulator.

The taper operation for this segment is functional.

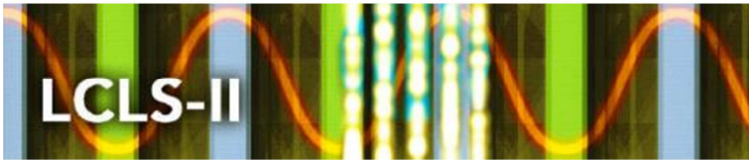


Gap Tapering– Matching Energy Loss

Generally, gap tapering will cause significant increases in the phase shake within the undulator segment. If however during high gain FEL operation the electrons loose significant amounts of energy, a matching gap taper can reduce the total phase shake to stay within the original parallel gap phase shake tolerance for constant energy.



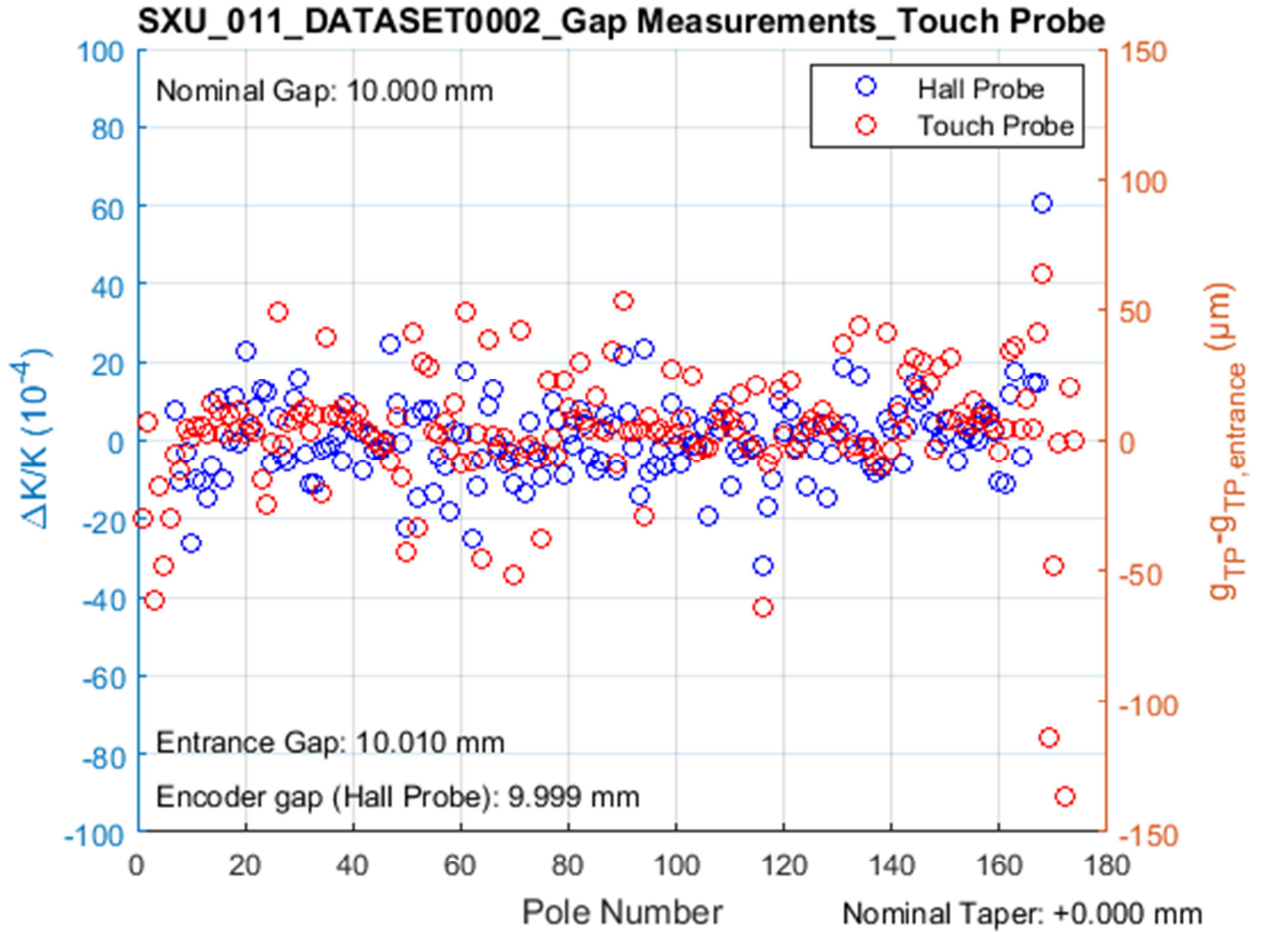
The upper figure shows a simplified linear energy loss function (Lorentz factor γ/γ_{Start}) optimized for the 0.3 mm gap taper at an 8 mm nominal gap. The lower figure shows the phase error along the undulator segment for the same parameters. The phase shake is only 1.6 degXray.



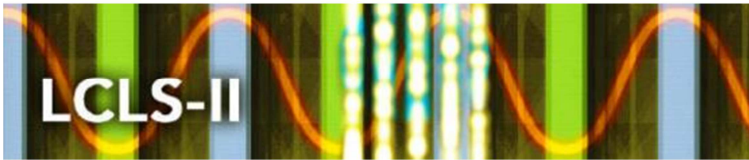
LCLS-II Undulator Segment Measurement Results

SXU-011

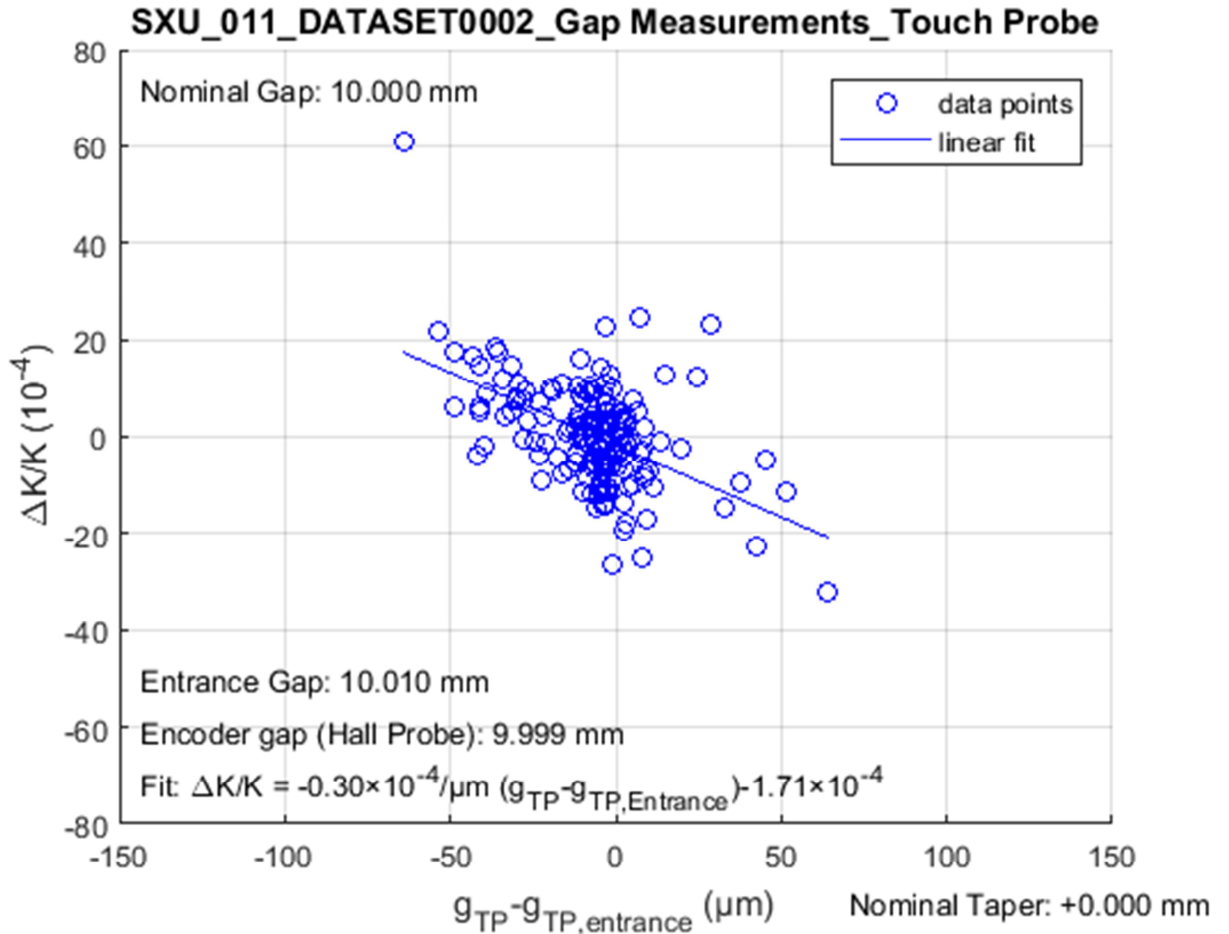
Touch Probe (TP) Analysis – Per pole gap vs per pole K (untapered)



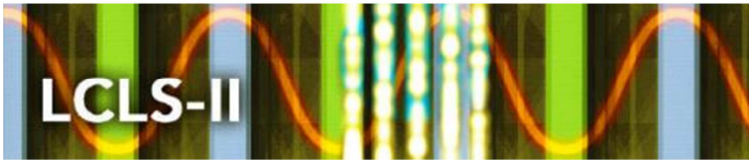
The figure shows $\Delta K/K$ (blue, left axis) (for the 162 core poles) as well as mechanical gap heights $\langle g_{TP} \rangle - g_{TP}$ (red, right axis) (for all 174 poles) based on touch probe measurements versus pole number. The large amplitude outliers are the result of tuning.



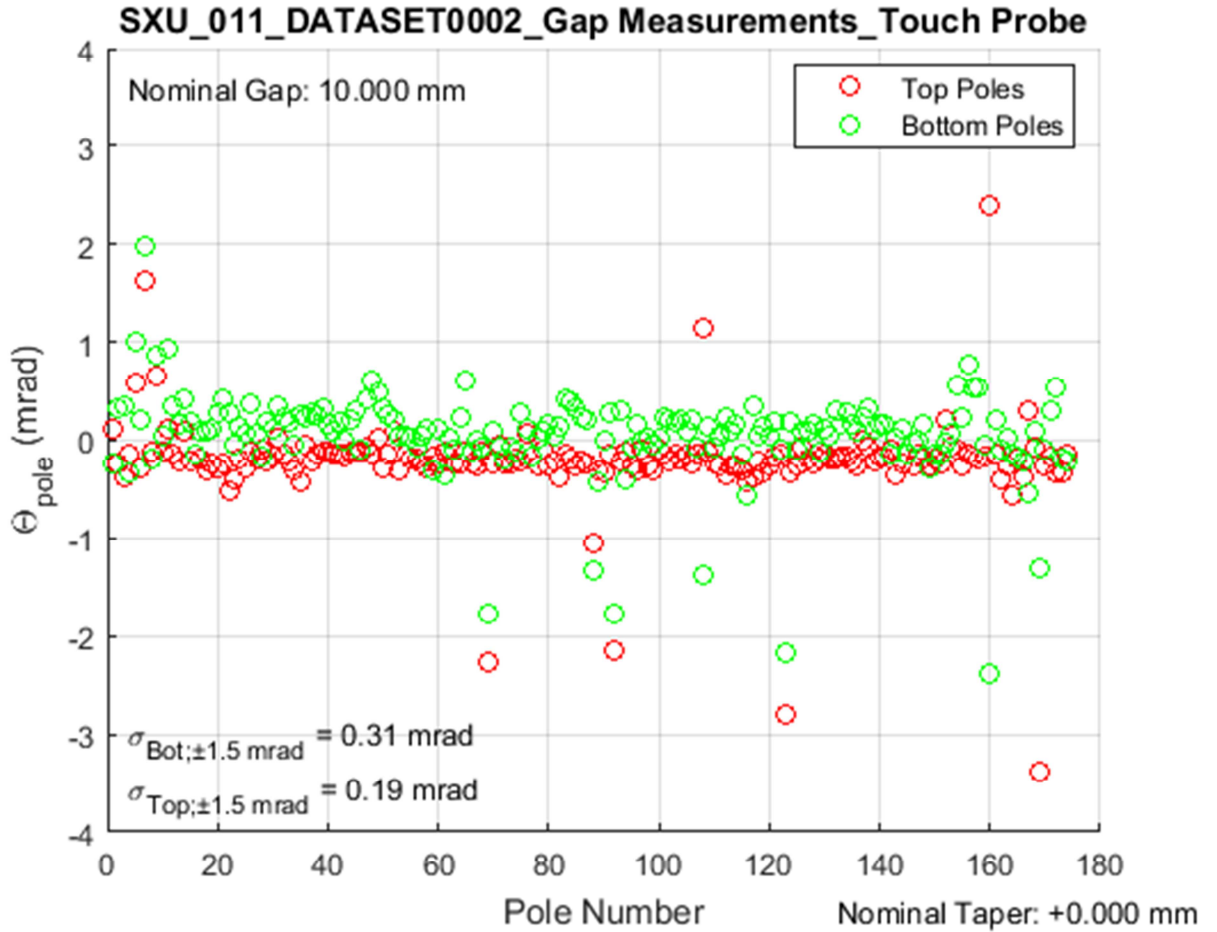
Touch Probe (TP) Analysis – K vs per pole gap (untapered)



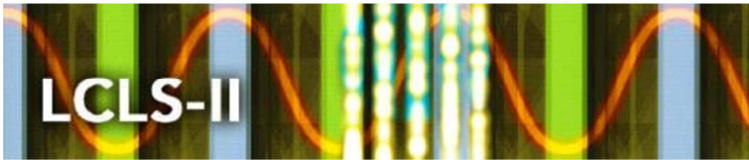
The figure shows the correlation between the $\Delta K_u / K_u$ for each pole from Hall probe measurements for the tuning gap and the deviation of the pole gap measured by the touch probe relative to its average (for the 164 core poles). The average gap measured with the touch probe and the one measured with the gap encoder are shown in the lower left corner of the figure. Also shown is the fit function.



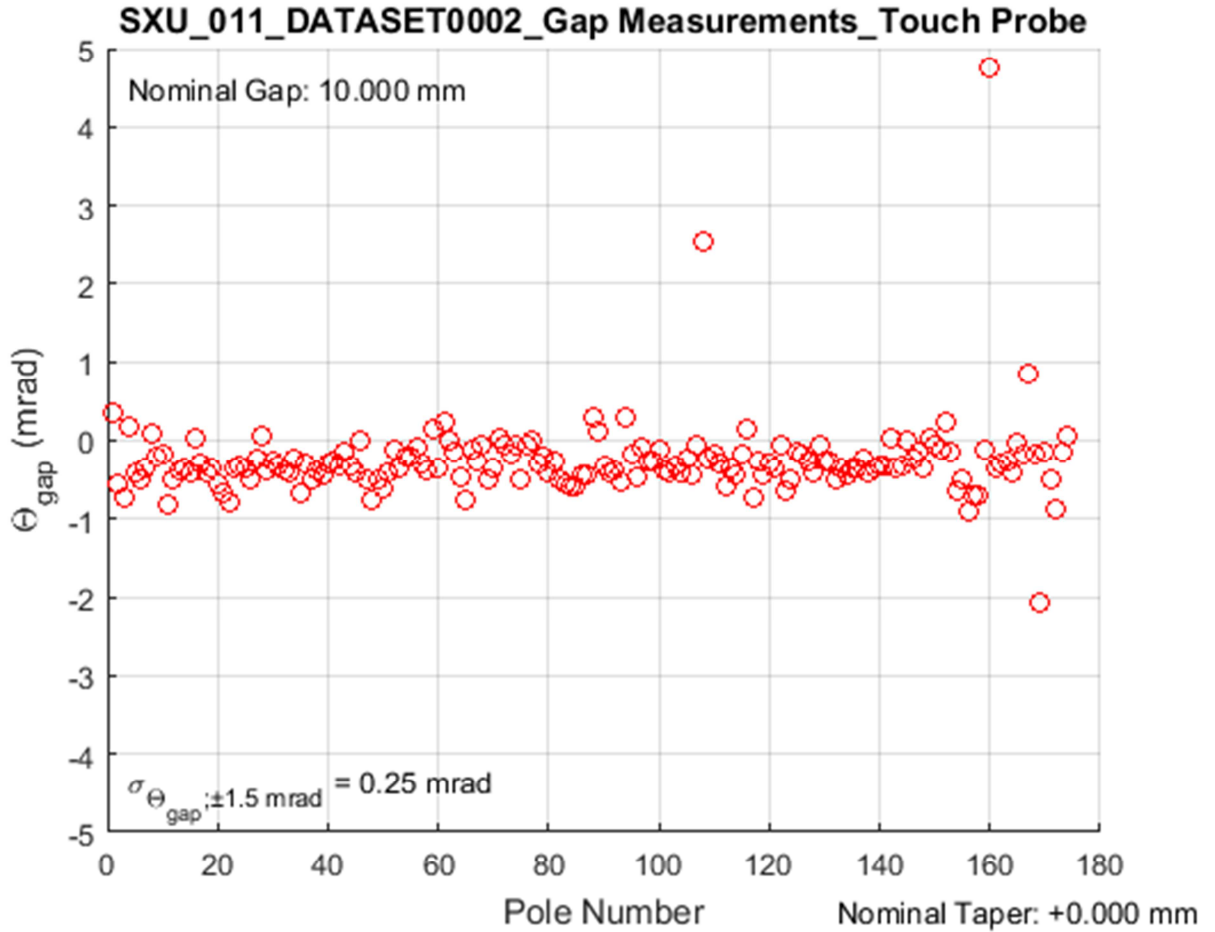
Touch Probe (TP) Analysis – Pole Cant Angles (untapered)



The figure shows the cant angles of each pole (top red, bottom green) relative to the horizontal plane defined by the Kugler bench at the Tuning Gap for all 174 poles, measured by the touch probe. The rms width of each distribution within a ± 1.5 mrad band is shown in the lower left corner of the figure. Note: that the distribution of the top pole angles is almost 3 times wider than that of the bottom pole angles. Not clear what the reason for this is.



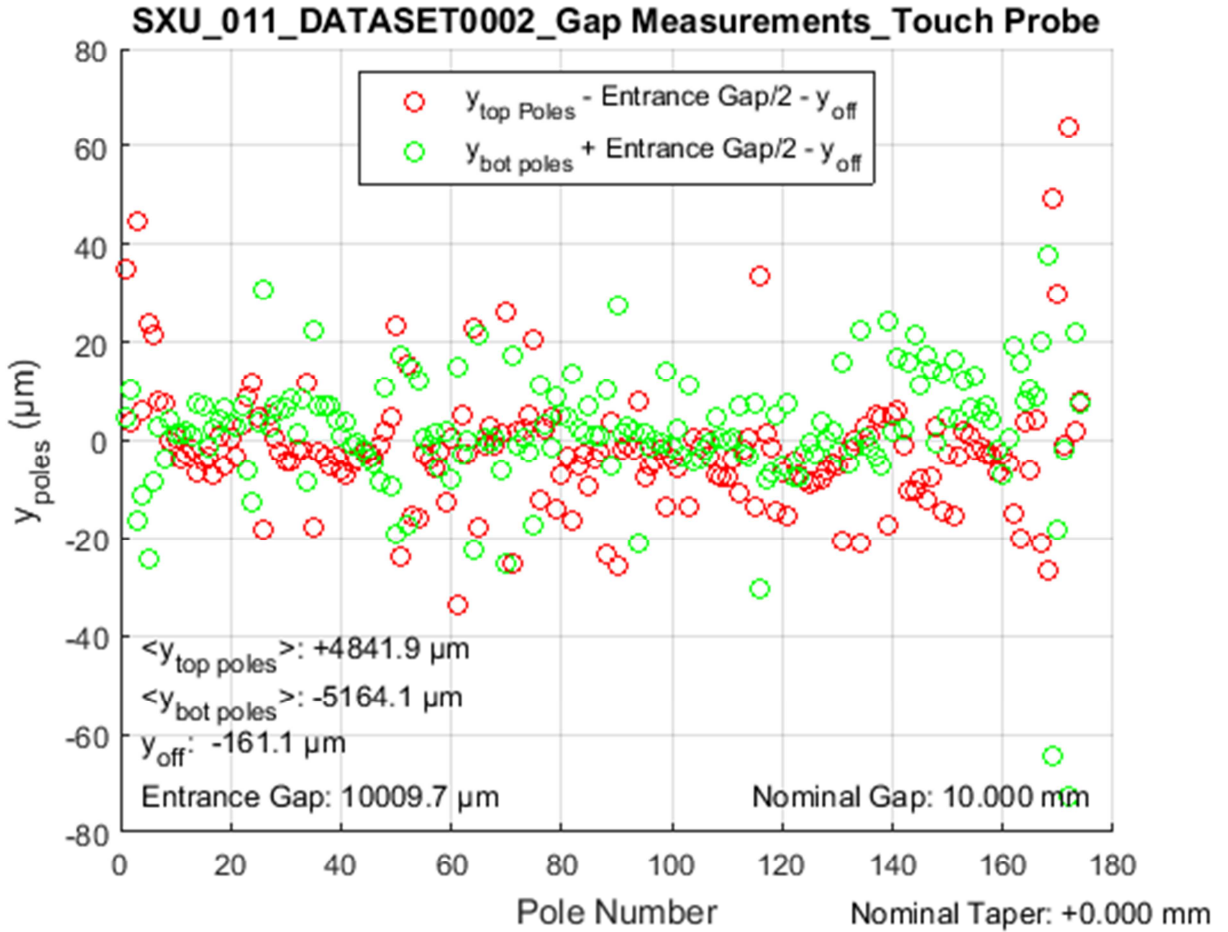
Touch Probe (TP) Analysis – Gap Cant Angles (untapered)



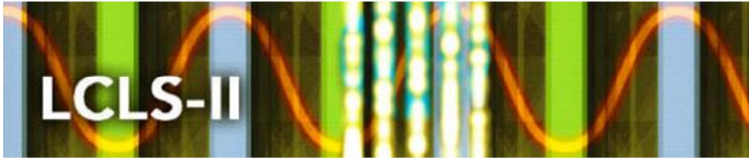
The figure shows the cant angles between the top and bottom part of each pole at the Tuning Gap for all 174 poles, measured by the touch probe. The rms width of the distribution within a ± 1.5 mrad band is shown in the lower left corner of the figure.



Touch Probe (TP) Analysis – Pole Heights (untapered)



The figure shows the relative vertical positions of the center of each pole (top red, bottom green) relative to the horizontal plane defined by the Kugler bench at the Tuning Gap for all 174 poles, measured by the touch probe.



LCLS-II Undulator Segment Measurement Results

SXU-011

Measurement Results are stored:

At V-Drive:

V:\MET\MagServe\MagData\LCLS-II\Undulator\

In Folder:

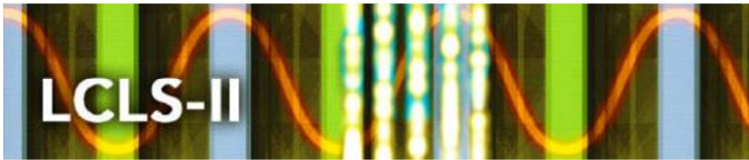
SXU_011\DATASET0002\Final Results\

Confirmation of File Locations:

The following lists all required data files documenting the tuning results. An existence check was done and the result is indicated next to each filename as “exists” or “missing”.

Sub folder: Z Scans\Good Field Region exists

001gap007.500x-01.00y+00.00\zscan.dat	exists
002gap007.500x-00.50y+00.00\zscan.dat	exists
003gap007.500x+00.00y+00.00\zscan.dat	exists
004gap007.500x+00.50y+00.00\zscan.dat	exists
005gap007.500x+01.00y+00.00\zscan.dat	exists
006gap007.500x+00.00y-00.50\zscan.dat	exists
003gap007.500x+00.00y+00.00\zscan.dat	exists
010gap007.500x+00.00y+00.50\zscan.dat	exists
011gap008.000x-01.00y+00.00\zscan.dat	exists
012gap008.000x-00.50y+00.00\zscan.dat	exists
013gap008.000x+00.00y+00.00\zscan.dat	exists
014gap008.000x+00.50y+00.00\zscan.dat	exists
015gap008.000x+01.00y+00.00\zscan.dat	exists
016gap008.000x+00.00y-00.50\zscan.dat	exists
013gap008.000x+00.00y+00.00\zscan.dat	exists
020gap008.000x+00.00y+00.50\zscan.dat	exists
021gap010.000x-01.00y+00.00\zscan.dat	exists
022gap010.000x-00.50y+00.00\zscan.dat	exists
023gap010.000x+00.00y+00.00\zscan.dat	exists



LCLS-II Undulator Segment Measurement Results

SXU-011

024gap010.000x+00.50y+00.00\zscan.dat	exists
025gap010.000x+01.00y+00.00\zscan.dat	exists
026gap010.000x+00.00y-00.50\zscan.dat	exists
023gap010.000x+00.00y+00.00\zscan.dat	exists
030gap010.000x+00.00y+00.50\zscan.dat	exists
031gap013.000x-01.00y+00.00\zscan.dat	exists
032gap013.000x-00.50y+00.00\zscan.dat	exists
033gap013.000x+00.00y+00.00\zscan.dat	exists
034gap013.000x+00.50y+00.00\zscan.dat	exists
035gap013.000x+01.00y+00.00\zscan.dat	exists
036gap013.000x+00.00y-00.50\zscan.dat	exists
033gap013.000x+00.00y+00.00\zscan.dat	exists
040gap013.000x+00.00y+00.50\zscan.dat	exists
041gap016.000x-01.00y+00.00\zscan.dat	exists
042gap016.000x-00.50y+00.00\zscan.dat	exists
043gap016.000x+00.00y+00.00\zscan.dat	exists
044gap016.000x+00.50y+00.00\zscan.dat	exists
045gap016.000x+01.00y+00.00\zscan.dat	exists
046gap016.000x+00.00y-00.50\zscan.dat	exists
043gap016.000x+00.00y+00.00\zscan.dat	exists
050gap016.000x+00.00y+00.50\zscan.dat	exists
051gap022.000x-01.00y+00.00\zscan.dat	exists
052gap022.000x-00.50y+00.00\zscan.dat	exists
053gap022.000x+00.00y+00.00\zscan.dat	exists
054gap022.000x+00.50y+00.00\zscan.dat	exists
055gap022.000x+01.00y+00.00\zscan.dat	exists
056gap022.000x+00.00y-00.50\zscan.dat	exists
053gap022.000x+00.00y+00.00\zscan.dat	exists
060gap022.000x+00.00y+00.50\zscan.dat	exists

Sub Folder: Z Scans\On Axis exists

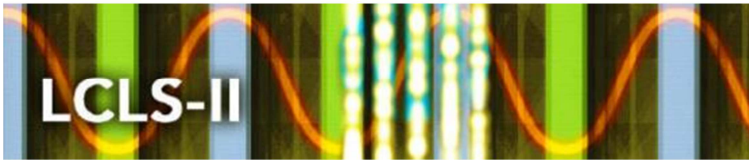
001gap007.200x+00.00y+00.00\zscan.dat	exists
003gap007.500x+00.00y+00.00\zscan.dat	exists
004gap007.750x+00.00y+00.00\zscan.dat	exists
005gap008.000x+00.00y+00.00\zscan.dat	exists
006gap008.250x+00.00y+00.00\zscan.dat	exists
007gap008.500x+00.00y+00.00\zscan.dat	exists
008gap008.750x+00.00y+00.00\zscan.dat	exists



LCLS-II Undulator Segment Measurement Results

SXU-011

009gap009.000x+00.00y+00.00\zscan.dat	exists
010gap009.250x+00.00y+00.00\zscan.dat	exists
011gap009.500x+00.00y+00.00\zscan.dat	exists
012gap009.750x+00.00y+00.00\zscan.dat	exists
013gap010.000x+00.00y+00.00\zscan.dat	exists
014gap010.250x+00.00y+00.00\zscan.dat	exists
015gap010.500x+00.00y+00.00\zscan.dat	exists
016gap010.750x+00.00y+00.00\zscan.dat	exists
017gap011.000x+00.00y+00.00\zscan.dat	exists
018gap011.500x+00.00y+00.00\zscan.dat	exists
019gap012.000x+00.00y+00.00\zscan.dat	exists
020gap012.500x+00.00y+00.00\zscan.dat	exists
021gap013.000x+00.00y+00.00\zscan.dat	exists
022gap013.500x+00.00y+00.00\zscan.dat	exists
023gap014.000x+00.00y+00.00\zscan.dat	exists
024gap014.500x+00.00y+00.00\zscan.dat	exists
025gap015.000x+00.00y+00.00\zscan.dat	exists
026gap015.500x+00.00y+00.00\zscan.dat	exists
027gap016.000x+00.00y+00.00\zscan.dat	exists
028gap016.500x+00.00y+00.00\zscan.dat	exists
029gap017.000x+00.00y+00.00\zscan.dat	exists
030gap017.500x+00.00y+00.00\zscan.dat	exists
031gap018.000x+00.00y+00.00\zscan.dat	exists
032gap018.500x+00.00y+00.00\zscan.dat	exists
033gap019.000x+00.00y+00.00\zscan.dat	exists
034gap019.500x+00.00y+00.00\zscan.dat	exists
035gap020.000x+00.00y+00.00\zscan.dat	exists
036gap020.500x+00.00y+00.00\zscan.dat	exists
037gap021.000x+00.00y+00.00\zscan.dat	exists
038gap021.500x+00.00y+00.00\zscan.dat	exists
039gap022.000x+00.00y+00.00\zscan.dat	exists
040gap023.000x+00.00y+00.00\zscan.dat	exists
041gap024.000x+00.00y+00.00\zscan.dat	exists
042gap025.000x+00.00y+00.00\zscan.dat	exists
043gap026.000x+00.00y+00.00\zscan.dat	exists
044gap027.000x+00.00y+00.00\zscan.dat	exists
045gap030.000x+00.00y+00.00\zscan.dat	exists
046gap040.000x+00.00y+00.00\zscan.dat	exists



LCLS-II Undulator Segment Measurement Results

SXU-011

047gap050.000x+00.00y+00.00\zscan.dat	exists
048gap060.000x+00.00y+00.00\zscan.dat	exists
049gap080.000x+00.00y+00.00\zscan.dat	exists
050gap100.000x+00.00y+00.00\zscan.dat	exists
051gap120.000x+00.00y+00.00\zscan.dat	exists
052gap140.000x+00.00y+00.00\zscan.dat	exists
053gap160.000x+00.00y+00.00\zscan.dat	exists
054gap180.000x+00.00y+00.00\zscan.dat	exists

Sub Folder: Z Scans\Commissioning Gap exists

001gap010.390x+00.00y+00.00\zscan.dat	exists
---------------------------------------	--------

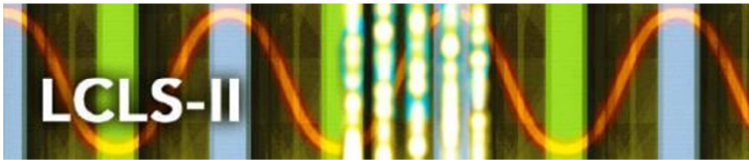
Sub Folder: Z Scans\Gap with taper exists

005gap010.000taper-0.100x+00.00y+00.00\zscan.dat	exists
007gap010.000taper+0.000x+00.00y+00.00\zscan.dat	exists
001gap010.000taper+0.100x+00.00y+00.00\zscan.dat	exists
003gap010.000taper+0.300x+00.00y+00.00\zscan.dat	exists
006gap020.000taper-0.100x+00.00y+00.00\zscan.dat	exists
008gap020.000taper+0.000x+00.00y+00.00\zscan.dat	exists
002gap020.000taper+0.100x+00.00y+00.00\zscan.dat	exists
004gap020.000taper+0.300x+00.00y+00.00\zscan.dat	exists

Sub Folder: Long Coil exists

Sub Folder: Long Coil\Good Field Region exists

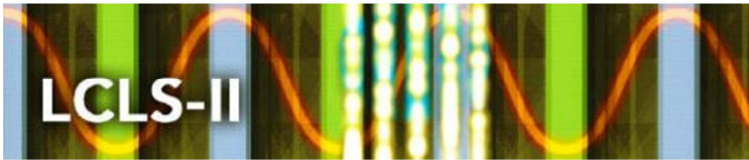
integrals_summary.txt	exists
011gap007.500x-01.00y+00.00_i1X_integrals.txt	exists
012gap007.500x-00.50y+00.00_i1X_integrals.txt	exists
013gap007.500x+00.00y+00.00_i1X_integrals.txt	exists
014gap007.500x+00.50y+00.00_i1X_integrals.txt	exists
015gap007.500x+01.00y+00.00_i1X_integrals.txt	exists
031gap007.500x+00.00y-01.00_i1X_integrals.txt	exists
035gap007.500x+00.00y+01.00_i1X_integrals.txt	exists
051gap008.000x-01.00y+00.00_i1X_integrals.txt	exists
052gap008.000x-00.50y+00.00_i1X_integrals.txt	exists
053gap008.000x+00.00y+00.00_i1X_integrals.txt	exists
054gap008.000x+00.50y+00.00_i1X_integrals.txt	exists



LCLS-II Undulator Segment Measurement Results

SXU-011

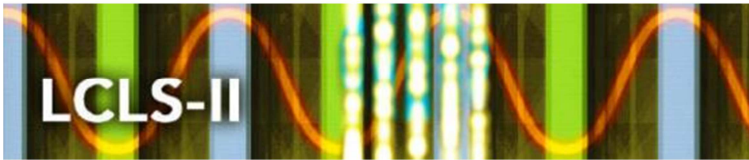
055gap008.000x+01.00y+00.00_i1X_integrals.txt	exists
071gap008.000x+00.00y-01.00_i1X_integrals.txt	exists
075gap008.000x+00.00y+01.00_i1X_integrals.txt	exists
091gap010.000x-01.00y+00.00_i1X_integrals.txt	exists
092gap010.000x-00.50y+00.00_i1X_integrals.txt	exists
093gap010.000x+00.00y+00.00_i1X_integrals.txt	exists
094gap010.000x+00.50y+00.00_i1X_integrals.txt	exists
095gap010.000x+01.00y+00.00_i1X_integrals.txt	exists
111gap010.000x+00.00y-01.00_i1X_integrals.txt	exists
115gap010.000x+00.00y+01.00_i1X_integrals.txt	exists
131gap013.000x-01.00y+00.00_i1X_integrals.txt	exists
132gap013.000x-00.50y+00.00_i1X_integrals.txt	exists
133gap013.000x+00.00y+00.00_i1X_integrals.txt	exists
134gap013.000x+00.50y+00.00_i1X_integrals.txt	exists
135gap013.000x+01.00y+00.00_i1X_integrals.txt	exists
151gap013.000x+00.00y-01.00_i1X_integrals.txt	exists
155gap013.000x+00.00y+01.00_i1X_integrals.txt	exists
171gap016.000x-01.00y+00.00_i1X_integrals.txt	exists
172gap016.000x-00.50y+00.00_i1X_integrals.txt	exists
173gap016.000x+00.00y+00.00_i1X_integrals.txt	exists
174gap016.000x+00.50y+00.00_i1X_integrals.txt	exists
175gap016.000x+01.00y+00.00_i1X_integrals.txt	exists
191gap016.000x+00.00y-01.00_i1X_integrals.txt	exists
195gap016.000x+00.00y+01.00_i1X_integrals.txt	exists
211gap022.000x-01.00y+00.00_i1X_integrals.txt	exists
212gap022.000x-00.50y+00.00_i1X_integrals.txt	exists
213gap022.000x+00.00y+00.00_i1X_integrals.txt	exists
214gap022.000x+00.50y+00.00_i1X_integrals.txt	exists
215gap022.000x+01.00y+00.00_i1X_integrals.txt	exists
231gap022.000x+00.00y-01.00_i1X_integrals.txt	exists
235gap022.000x+00.00y+01.00_i1X_integrals.txt	exists
251gap100.000x-01.00y+00.00_i1X_integrals.txt	exists
252gap100.000x-00.50y+00.00_i1X_integrals.txt	exists
253gap100.000x+00.00y+00.00_i1X_integrals.txt	exists
254gap100.000x+00.50y+00.00_i1X_integrals.txt	exists
255gap100.000x+01.00y+00.00_i1X_integrals.txt	exists
271gap100.000x+00.00y-01.00_i1X_integrals.txt	exists
275gap100.000x+00.00y+01.00_i1X_integrals.txt	exists



LCLS-II Undulator Segment Measurement Results

SXU-011

016gap007.500x-01.00y+00.00_i2X_integrals.txt	exists
017gap007.500x-00.50y+00.00_i2X_integrals.txt	exists
018gap007.500x+00.00y+00.00_i2X_integrals.txt	exists
019gap007.500x+00.50y+00.00_i2X_integrals.txt	exists
020gap007.500x+01.00y+00.00_i2X_integrals.txt	exists
036gap007.500x+00.00y-01.00_i2X_integrals.txt	exists
040gap007.500x+00.00y+01.00_i2X_integrals.txt	exists
056gap008.000x-01.00y+00.00_i2X_integrals.txt	exists
057gap008.000x-00.50y+00.00_i2X_integrals.txt	exists
058gap008.000x+00.00y+00.00_i2X_integrals.txt	exists
059gap008.000x+00.50y+00.00_i2X_integrals.txt	exists
060gap008.000x+01.00y+00.00_i2X_integrals.txt	exists
076gap008.000x+00.00y-01.00_i2X_integrals.txt	exists
080gap008.000x+00.00y+01.00_i2X_integrals.txt	exists
096gap010.000x-01.00y+00.00_i2X_integrals.txt	exists
097gap010.000x-00.50y+00.00_i2X_integrals.txt	exists
098gap010.000x+00.00y+00.00_i2X_integrals.txt	exists
099gap010.000x+00.50y+00.00_i2X_integrals.txt	exists
100gap010.000x+01.00y+00.00_i2X_integrals.txt	exists
116gap010.000x+00.00y-01.00_i2X_integrals.txt	exists
120gap010.000x+00.00y+01.00_i2X_integrals.txt	exists
136gap013.000x-01.00y+00.00_i2X_integrals.txt	exists
137gap013.000x-00.50y+00.00_i2X_integrals.txt	exists
138gap013.000x+00.00y+00.00_i2X_integrals.txt	exists
139gap013.000x+00.50y+00.00_i2X_integrals.txt	exists
140gap013.000x+01.00y+00.00_i2X_integrals.txt	exists
156gap013.000x+00.00y-01.00_i2X_integrals.txt	exists
160gap013.000x+00.00y+01.00_i2X_integrals.txt	exists
176gap016.000x-01.00y+00.00_i2X_integrals.txt	exists
177gap016.000x-00.50y+00.00_i2X_integrals.txt	exists
178gap016.000x+00.00y+00.00_i2X_integrals.txt	exists
179gap016.000x+00.50y+00.00_i2X_integrals.txt	exists
180gap016.000x+01.00y+00.00_i2X_integrals.txt	exists
196gap016.000x+00.00y-01.00_i2X_integrals.txt	exists
200gap016.000x+00.00y+01.00_i2X_integrals.txt	exists
216gap022.000x-01.00y+00.00_i2X_integrals.txt	exists
217gap022.000x-00.50y+00.00_i2X_integrals.txt	exists
218gap022.000x+00.00y+00.00_i2X_integrals.txt	exists



LCLS-II Undulator Segment Measurement Results

SXU-011

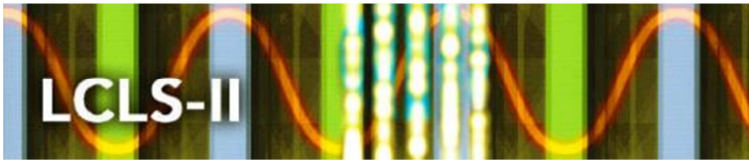
219gap022.000x+00.50y+00.00_i2X_integrals.txt	exists
220gap022.000x+01.00y+00.00_i2X_integrals.txt	exists
236gap022.000x+00.00y-01.00_i2X_integrals.txt	exists
240gap022.000x+00.00y+01.00_i2X_integrals.txt	exists
256gap100.000x-01.00y+00.00_i2X_integrals.txt	exists
257gap100.000x-00.50y+00.00_i2X_integrals.txt	exists
258gap100.000x+00.00y+00.00_i2X_integrals.txt	exists
259gap100.000x+00.50y+00.00_i2X_integrals.txt	exists
260gap100.000x+01.00y+00.00_i2X_integrals.txt	exists
276gap100.000x+00.00y-01.00_i2X_integrals.txt	exists
280gap100.000x+00.00y+01.00_i2X_integrals.txt	exists
001gap007.500x-01.00y+00.00_i1Y_integrals.txt	exists
002gap007.500x-00.50y+00.00_i1Y_integrals.txt	exists
003gap007.500x+00.00y+00.00_i1Y_integrals.txt	exists
004gap007.500x+00.50y+00.00_i1Y_integrals.txt	exists
005gap007.500x+01.00y+00.00_i1Y_integrals.txt	exists
021gap007.500x+00.00y-01.00_i1Y_integrals.txt	exists
025gap007.500x+00.00y+01.00_i1Y_integrals.txt	exists
041gap008.000x-01.00y+00.00_i1Y_integrals.txt	exists
042gap008.000x-00.50y+00.00_i1Y_integrals.txt	exists
043gap008.000x+00.00y+00.00_i1Y_integrals.txt	exists
044gap008.000x+00.50y+00.00_i1Y_integrals.txt	exists
045gap008.000x+01.00y+00.00_i1Y_integrals.txt	exists
061gap008.000x+00.00y-01.00_i1Y_integrals.txt	exists
065gap008.000x+00.00y+01.00_i1Y_integrals.txt	exists
081gap010.000x-01.00y+00.00_i1Y_integrals.txt	exists
082gap010.000x-00.50y+00.00_i1Y_integrals.txt	exists
083gap010.000x+00.00y+00.00_i1Y_integrals.txt	exists
084gap010.000x+00.50y+00.00_i1Y_integrals.txt	exists
085gap010.000x+01.00y+00.00_i1Y_integrals.txt	exists
101gap010.000x+00.00y-01.00_i1Y_integrals.txt	exists
105gap010.000x+00.00y+01.00_i1Y_integrals.txt	exists
121gap013.000x-01.00y+00.00_i1Y_integrals.txt	exists
122gap013.000x-00.50y+00.00_i1Y_integrals.txt	exists
123gap013.000x+00.00y+00.00_i1Y_integrals.txt	exists
124gap013.000x+00.50y+00.00_i1Y_integrals.txt	exists
125gap013.000x+01.00y+00.00_i1Y_integrals.txt	exists
141gap013.000x+00.00y-01.00_i1Y_integrals.txt	exists



LCLS-II Undulator Segment Measurement Results

SXU-011

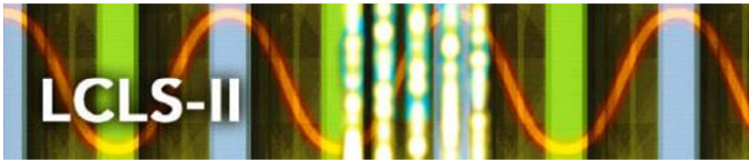
145gap013.000x+00.00y+01.00_i1Y_integrals.txt	exists
161gap016.000x-01.00y+00.00_i1Y_integrals.txt	exists
162gap016.000x-00.50y+00.00_i1Y_integrals.txt	exists
163gap016.000x+00.00y+00.00_i1Y_integrals.txt	exists
164gap016.000x+00.50y+00.00_i1Y_integrals.txt	exists
165gap016.000x+01.00y+00.00_i1Y_integrals.txt	exists
181gap016.000x+00.00y-01.00_i1Y_integrals.txt	exists
185gap016.000x+00.00y+01.00_i1Y_integrals.txt	exists
201gap022.000x-01.00y+00.00_i1Y_integrals.txt	exists
202gap022.000x-00.50y+00.00_i1Y_integrals.txt	exists
203gap022.000x+00.00y+00.00_i1Y_integrals.txt	exists
204gap022.000x+00.50y+00.00_i1Y_integrals.txt	exists
205gap022.000x+01.00y+00.00_i1Y_integrals.txt	exists
221gap022.000x+00.00y-01.00_i1Y_integrals.txt	exists
225gap022.000x+00.00y+01.00_i1Y_integrals.txt	exists
241gap100.000x-01.00y+00.00_i1Y_integrals.txt	exists
242gap100.000x-00.50y+00.00_i1Y_integrals.txt	exists
243gap100.000x+00.00y+00.00_i1Y_integrals.txt	exists
244gap100.000x+00.50y+00.00_i1Y_integrals.txt	exists
245gap100.000x+01.00y+00.00_i1Y_integrals.txt	exists
261gap100.000x+00.00y-01.00_i1Y_integrals.txt	exists
265gap100.000x+00.00y+01.00_i1Y_integrals.txt	exists
006gap007.500x-01.00y+00.00_i2Y_integrals.txt	exists
007gap007.500x-00.50y+00.00_i2Y_integrals.txt	exists
008gap007.500x+00.00y+00.00_i2Y_integrals.txt	exists
009gap007.500x+00.50y+00.00_i2Y_integrals.txt	exists
010gap007.500x+01.00y+00.00_i2Y_integrals.txt	exists
026gap007.500x+00.00y-01.00_i2Y_integrals.txt	exists
030gap007.500x+00.00y+01.00_i2Y_integrals.txt	exists
046gap008.000x-01.00y+00.00_i2Y_integrals.txt	exists
047gap008.000x-00.50y+00.00_i2Y_integrals.txt	exists
048gap008.000x+00.00y+00.00_i2Y_integrals.txt	exists
049gap008.000x+00.50y+00.00_i2Y_integrals.txt	exists
050gap008.000x+01.00y+00.00_i2Y_integrals.txt	exists
066gap008.000x+00.00y-01.00_i2Y_integrals.txt	exists
070gap008.000x+00.00y+01.00_i2Y_integrals.txt	exists
086gap010.000x-01.00y+00.00_i2Y_integrals.txt	exists
087gap010.000x-00.50y+00.00_i2Y_integrals.txt	exists



LCLS-II Undulator Segment Measurement Results

SXU-011

088gap010.000x+00.00y+00.00_i2Y_integrals.txt	exists
089gap010.000x+00.50y+00.00_i2Y_integrals.txt	exists
090gap010.000x+01.00y+00.00_i2Y_integrals.txt	exists
106gap010.000x+00.00y-01.00_i2Y_integrals.txt	exists
110gap010.000x+00.00y+01.00_i2Y_integrals.txt	exists
126gap013.000x-01.00y+00.00_i2Y_integrals.txt	exists
127gap013.000x-00.50y+00.00_i2Y_integrals.txt	exists
128gap013.000x+00.00y+00.00_i2Y_integrals.txt	exists
129gap013.000x+00.50y+00.00_i2Y_integrals.txt	exists
130gap013.000x+01.00y+00.00_i2Y_integrals.txt	exists
146gap013.000x+00.00y-01.00_i2Y_integrals.txt	exists
150gap013.000x+00.00y+01.00_i2Y_integrals.txt	exists
166gap016.000x-01.00y+00.00_i2Y_integrals.txt	exists
167gap016.000x-00.50y+00.00_i2Y_integrals.txt	exists
168gap016.000x+00.00y+00.00_i2Y_integrals.txt	exists
169gap016.000x+00.50y+00.00_i2Y_integrals.txt	exists
170gap016.000x+01.00y+00.00_i2Y_integrals.txt	exists
186gap016.000x+00.00y-01.00_i2Y_integrals.txt	exists
190gap016.000x+00.00y+01.00_i2Y_integrals.txt	exists
206gap022.000x-01.00y+00.00_i2Y_integrals.txt	exists
207gap022.000x-00.50y+00.00_i2Y_integrals.txt	exists
208gap022.000x+00.00y+00.00_i2Y_integrals.txt	exists
209gap022.000x+00.50y+00.00_i2Y_integrals.txt	exists
210gap022.000x+01.00y+00.00_i2Y_integrals.txt	exists
226gap022.000x+00.00y-01.00_i2Y_integrals.txt	exists
230gap022.000x+00.00y+01.00_i2Y_integrals.txt	exists
246gap100.000x-01.00y+00.00_i2Y_integrals.txt	exists
247gap100.000x-00.50y+00.00_i2Y_integrals.txt	exists
248gap100.000x+00.00y+00.00_i2Y_integrals.txt	exists
249gap100.000x+00.50y+00.00_i2Y_integrals.txt	exists
250gap100.000x+01.00y+00.00_i2Y_integrals.txt	exists
266gap100.000x+00.00y-01.00_i2Y_integrals.txt	exists
270gap100.000x+00.00y+01.00_i2Y_integrals.txt	exists

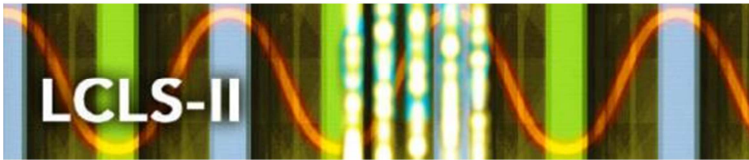


LCLS-II Undulator Segment Measurement Results

SXU-011

Sub Folder: Long Coil\On Axis exists

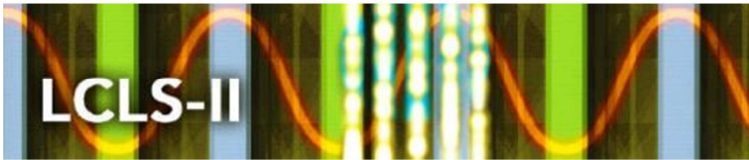
integrals_summary.txt	exists
003gap007.200x+00.00y+00.00_i1X_integrals.txt	exists
004gap007.200x+00.00y+00.00_i2X_integrals.txt	exists
001gap007.200x+00.00y+00.00_i1Y_integrals.txt	exists
002gap007.200x+00.00y+00.00_i2Y_integrals.txt	exists
007gap007.500x+00.00y+00.00_i1X_integrals.txt	exists
008gap007.500x+00.00y+00.00_i2X_integrals.txt	exists
005gap007.500x+00.00y+00.00_i1Y_integrals.txt	exists
006gap007.500x+00.00y+00.00_i2Y_integrals.txt	exists
011gap008.000x+00.00y+00.00_i1X_integrals.txt	exists
012gap008.000x+00.00y+00.00_i2X_integrals.txt	exists
009gap008.000x+00.00y+00.00_i1Y_integrals.txt	exists
010gap008.000x+00.00y+00.00_i2Y_integrals.txt	exists
015gap008.500x+00.00y+00.00_i1X_integrals.txt	exists
016gap008.500x+00.00y+00.00_i2X_integrals.txt	exists
013gap008.500x+00.00y+00.00_i1Y_integrals.txt	exists
014gap008.500x+00.00y+00.00_i2Y_integrals.txt	exists
019gap009.000x+00.00y+00.00_i1X_integrals.txt	exists
020gap009.000x+00.00y+00.00_i2X_integrals.txt	exists
017gap009.000x+00.00y+00.00_i1Y_integrals.txt	exists
018gap009.000x+00.00y+00.00_i2Y_integrals.txt	exists
027gap010.000x+00.00y+00.00_i1X_integrals.txt	exists
028gap010.000x+00.00y+00.00_i2X_integrals.txt	exists
025gap010.000x+00.00y+00.00_i1Y_integrals.txt	exists
026gap010.000x+00.00y+00.00_i2Y_integrals.txt	exists
035gap012.000x+00.00y+00.00_i1X_integrals.txt	exists
036gap012.000x+00.00y+00.00_i2X_integrals.txt	exists
033gap012.000x+00.00y+00.00_i1Y_integrals.txt	exists
034gap012.000x+00.00y+00.00_i2Y_integrals.txt	exists
043gap014.000x+00.00y+00.00_i1X_integrals.txt	exists
044gap014.000x+00.00y+00.00_i2X_integrals.txt	exists
041gap014.000x+00.00y+00.00_i1Y_integrals.txt	exists
042gap014.000x+00.00y+00.00_i2Y_integrals.txt	exists
047gap016.000x+00.00y+00.00_i1X_integrals.txt	exists
048gap016.000x+00.00y+00.00_i2X_integrals.txt	exists
045gap016.000x+00.00y+00.00_i1Y_integrals.txt	exists



LCLS-II Undulator Segment Measurement Results

SXU-011

046gap016.000x+00.00y+00.00_i2Y_integrals.txt	exists
051gap018.000x+00.00y+00.00_i1X_integrals.txt	exists
052gap018.000x+00.00y+00.00_i2X_integrals.txt	exists
049gap018.000x+00.00y+00.00_i1Y_integrals.txt	exists
050gap018.000x+00.00y+00.00_i2Y_integrals.txt	exists
055gap020.000x+00.00y+00.00_i1X_integrals.txt	exists
056gap020.000x+00.00y+00.00_i2X_integrals.txt	exists
053gap020.000x+00.00y+00.00_i1Y_integrals.txt	exists
054gap020.000x+00.00y+00.00_i2Y_integrals.txt	exists
059gap022.000x+00.00y+00.00_i1X_integrals.txt	exists
060gap022.000x+00.00y+00.00_i2X_integrals.txt	exists
057gap022.000x+00.00y+00.00_i1Y_integrals.txt	exists
058gap022.000x+00.00y+00.00_i2Y_integrals.txt	exists
063gap025.000x+00.00y+00.00_i1X_integrals.txt	exists
064gap025.000x+00.00y+00.00_i2X_integrals.txt	exists
061gap025.000x+00.00y+00.00_i1Y_integrals.txt	exists
062gap025.000x+00.00y+00.00_i2Y_integrals.txt	exists
067gap030.000x+00.00y+00.00_i1X_integrals.txt	exists
068gap030.000x+00.00y+00.00_i2X_integrals.txt	exists
065gap030.000x+00.00y+00.00_i1Y_integrals.txt	exists
066gap030.000x+00.00y+00.00_i2Y_integrals.txt	exists
071gap040.000x+00.00y+00.00_i1X_integrals.txt	exists
072gap040.000x+00.00y+00.00_i2X_integrals.txt	exists
069gap040.000x+00.00y+00.00_i1Y_integrals.txt	exists
070gap040.000x+00.00y+00.00_i2Y_integrals.txt	exists
075gap050.000x+00.00y+00.00_i1X_integrals.txt	exists
076gap050.000x+00.00y+00.00_i2X_integrals.txt	exists
073gap050.000x+00.00y+00.00_i1Y_integrals.txt	exists
074gap050.000x+00.00y+00.00_i2Y_integrals.txt	exists
079gap060.000x+00.00y+00.00_i1X_integrals.txt	exists
080gap060.000x+00.00y+00.00_i2X_integrals.txt	exists
077gap060.000x+00.00y+00.00_i1Y_integrals.txt	exists
078gap060.000x+00.00y+00.00_i2Y_integrals.txt	exists
083gap080.000x+00.00y+00.00_i1X_integrals.txt	exists
084gap080.000x+00.00y+00.00_i2X_integrals.txt	exists
081gap080.000x+00.00y+00.00_i1Y_integrals.txt	exists
082gap080.000x+00.00y+00.00_i2Y_integrals.txt	exists
087gap100.000x+00.00y+00.00_i1X_integrals.txt	exists



LCLS-II Undulator Segment Measurement Results

SXU-011

088gap100.000x+00.00y+00.00_i2X_integrals.txt	exists
085gap100.000x+00.00y+00.00_i1Y_integrals.txt	exists
086gap100.000x+00.00y+00.00_i2Y_integrals.txt	exists
091gap120.000x+00.00y+00.00_i1X_integrals.txt	exists
092gap120.000x+00.00y+00.00_i2X_integrals.txt	exists
089gap120.000x+00.00y+00.00_i1Y_integrals.txt	exists
090gap120.000x+00.00y+00.00_i2Y_integrals.txt	exists
095gap140.000x+00.00y+00.00_i1X_integrals.txt	exists
096gap140.000x+00.00y+00.00_i2X_integrals.txt	exists
093gap140.000x+00.00y+00.00_i1Y_integrals.txt	exists
094gap140.000x+00.00y+00.00_i2Y_integrals.txt	exists
099gap160.000x+00.00y+00.00_i1X_integrals.txt	exists
100gap160.000x+00.00y+00.00_i2X_integrals.txt	exists
097gap160.000x+00.00y+00.00_i1Y_integrals.txt	exists
098gap160.000x+00.00y+00.00_i2Y_integrals.txt	exists
103gap180.000x+00.00y+00.00_i1X_integrals.txt	exists
104gap180.000x+00.00y+00.00_i2X_integrals.txt	exists
101gap180.000x+00.00y+00.00_i1Y_integrals.txt	exists
102gap180.000x+00.00y+00.00_i2Y_integrals.txt	exists

Sub Folder: Fiducialization exists

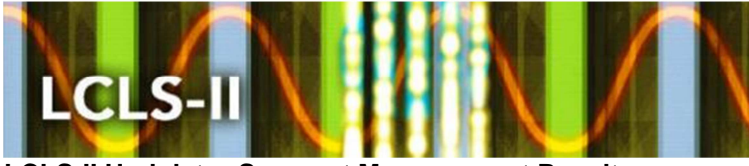
LCLS2 SXU 011 Fiducial Report.docx	exists
------------------------------------	--------

Sub Folder: Gap Measurements exists

Sub Folder: Gap Measurements\Touch Probe exists

001gap010.000taper-0.100.pdf	exists
001gap010.000taper-0.100.txt	exists
004gap010.000taper+0.000.pdf	exists
004gap010.000taper+0.000.txt	exists
002gap010.000taper+0.100.pdf	exists
002gap010.000taper+0.100.txt	exists
003gap010.000taper+0.300.pdf	exists
003gap010.000taper+0.300.txt	exists

Sub Folder: Gap Measurements\Capacitive Sensors exists



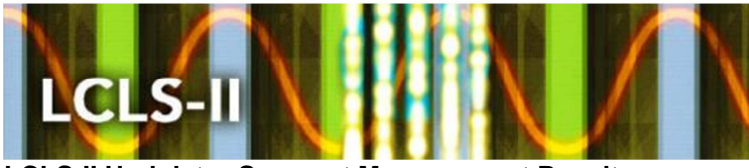
LCLS-II Undulator Segment Measurement Results

SXU-011

gap_dat_ru1.dat	exists
-----------------	--------

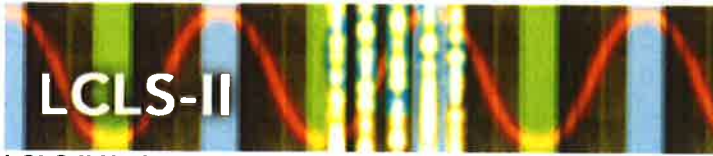
Sub Folder: Controls Data exists

sxu_011_parameters.txt	exists
sxu_011_k_vs_gap_spline.dat	exists
sxu_011_phase_match_enter_vs_gap_spline.dat	exists
sxu_011_phase_match_exit_vs_gap_spline.dat	exists
sxu_011_yctr_vs_gap_spline.dat	exists
sxu_011_i1xvsgap_spline.dat	exists
sxu_011_i1yvsgap_spline.dat	exists
sxu_011_i2xvsgap_spline.dat	exists
sxu_011_i2yvsgap_spline.dat	exists



LCLS-II Undulator Segment Measurement Results

SXU-011



LCLS-II Undulator Segment Measurement Results

SXU-011

Summary of findings

Finding	Solution

Approval and Assignment by Heinz-Dieter Nuhn:

Data Storage Checked:	Y	Y/N
Magnet accepted:	Y	Y/N
Assigned Location	SXU-011	

	Heinz-Dieter Nuhn	8/20/21018
(Signature)	(Name)	(Date)